

## **Reply letter to the anonymous Referee #1**

Received and published: 14 September 2016

The paper aimed at the severe haze events during the winter of 2014 happened in North-Central North China Plain, in which the authors attributed the main cause of haze in 2014 winter to the positive phases of the three teleconnection patterns: the East Atlantic/West Russia (EA/WR), the Western Pacific (WP), and the Eurasia (EU). The authors supplied some correlation analysis to explain the influences of three patterns to haze days over the North-Central North China Plain ( $WHD_{NCP}$ ), and they put the results of SVD to illustrate the causes of three patterns in 2014. The severe haze events in China has become a hotspot in the research of atmospheric environment, thus the issue of this paper is interesting, as documented by some other papers in recent years. **This paper pointed out the three patterns of teleconnection exerted important effects to haze days in China in 2014, and there are some other papers raised similar view of atmospheric circulation, therefore, there is not enough novelty in this paper.**

### ***Reply:***

Since several years ago, we have been working on the impact of climate change on the haze pollution in China (associated publications were listed below) and keeping tracking the related researches. We confirmed that this study had some new and key progress, such as:

- (1) We investigated the joint effects of the EA/WR, EU and WP teleconnection patterns for the first time and pointed out the pivotal role of the anomalous high over North China.
- (2) The latest extremes of haze days in 2010, 2013 and 2014 were analyzed. Not from a specific perspective, but the comprehensive climate conditions (i.e., the related anomalous circulations and external forcings) were researched.
- (3) By comparing 2010 and 2014, we confirmed both local climate conditions and climate teleconnections influenced haze weather very much.
- (4) Furthermore, the reconstructed haze dataset based on meteorological observations

agree well with the atmospheric composition measurements (particularly the GAWS), thus providing a basis for long-term variability study on the haze pollution.

#### *Associated publications*

1. Chen H. P., and **H. J. Wang**, 2015: Haze days in North China and the associated atmospheric circulations based on daily visibility data from 1960 to 2012. *J. Geophys. Res. Atmos.*, 120, 5895-5909, doi:10.1002/2015JD023225.
2. **Wang H. J.**, H. P. Chen, and J. Liu, 2015: Arctic sea ice decline intensified haze pollution in eastern China. *Atmos. Oceanic Sci. Lett.*, 8, 1-9.
3. **Wang H. J.**, H. P. Chen. 2016: Understanding the recent trend of haze pollution in eastern China: roles of climate change. *Atmos. Chem. Phys.*, 16, 4205—4211
4. **Yin Z. C.**, **H. J. Wang**, 2015: The relationship between the subtropical Western Pacific SST and haze over North-Central North China Plain. *Int. J. Climatol.*, doi:10.1002/joc.4570.
5. **Yin Z. C.**, **H. J. Wang**, W. L. Guo, 2015: Climatic change features of fog and haze in winter over North China and Huang-Huai Area. *SCIENCE CHINA EarthSciences*, 58(8): 1370-1376.
6. **Yin Z. C.**, **H. J. Wang**, D. M. Yuan, 2015: Interdecadal increase of haze in winter over North China and the Huang-huai Area and the weakening of the East Asia Winter Monsoon, *Chin Sci Bull*, 2015, 60: 1395–1400 (in Chinese).
7. **Yin, Z. and Wang, H.**: Seasonal Prediction of Winter Haze Days in the North-Central North China Plain, *Atmos. Chem. Phys.*, doi:10.5194/acp-2016-691, accepted, 2016.

**1, The WHD<sub>NCP</sub> shown in Fig. 4 includes significantly spatial changes in the research domain, and the domain is very small with respect to the spatial scales of three patterns. How can the authors explain the difference of WHD<sub>NCP</sub> in such a little region using so large three patterns?**

**Reply:**

**Due to the influence of human activities, the distribution of WHD shows significantly spatial changes among the rural area, small cities and metropolises.**

In the paper, we supplemented some analysis about the rural stations in Figure 1. From the Figure 1 and 2a, we can see that the areas with less WHD were near the rural stations. Actually, the increase of WHD in rural area was an obvious reflection of the severe haze disaster in recent years. In other words, **the coverage of haze invaded into the rural region in 2014.**

We found that **large scale patterns could impact the haze events in the relatively small region by altering the local meteorological conditions via teleconnection** (i.e., EA/WR teleconnection pattern, WP teleconnection pattern and EU teleconnection pattern). For example, when the WP pattern showed stronger positive phase, there were stronger positive anomalies of geopotential height on surface, 850 hPa and 500 hPa over North China and northwest Pacific. The anomalous anti-cyclone was enhanced, thus, the vertical motion or convection on the NCP was confined and the southerly anomalies on the left side of the anti-cyclone were induced to weaken the cold air and wind speed. This is the way that the WP teleconnection pattern altered the local meteorological conditions. Under such meteorological conditions, the vertical and horizontal diffusions of atmospheric particulates were both restricted, and then the pollutant gathered in a narrow space that resulted in the occurrence of haze. **The main process could be summarized as “climate teleconnection → local climate conditions → weaker diffusion conditions → pollutant gathered in a narrow space”.** The physical process related with EA/WR and EU were similar to that was described above. The Figures 4—5 was revised and the order was exchanged to match the improvement of the physical analysis. The revised text and Figures was showed in the replies to “Specific comment 2”.

Additionally, the impact of ENSO (Gao et al. 2015) and Tibetan Plateau (Xu et al. 2016) on the haze frequency in eastern China was also obvious, whose scales were even larger. What’s more, the North China severe summer drought in 2014 also been

explained by the large scale teleconnections (Wang et al. 2015).

*Associated references*

Wang H J, He S P. 2015. The North China/Northeastern Asia Severe Summer Drought in 2014. *Journal of Climate*. 28(17), 6667–668

Gao H, Li X. 2015. Influences of El Nino Southern Oscillation events on haze frequency in eastern China during boreal winters. *International Journal of Climatology*. 35

Xu X et al. 2016. Climate modulation of the Tibetan Plateau on haze in China. *Atmospheric Chemistry and Physics*, 16(3): 1365-1375

**Revision:**

.....Due to the quality and temporal range of the data, only four rural stations were qualified and selected (white circles in Figure 1).....

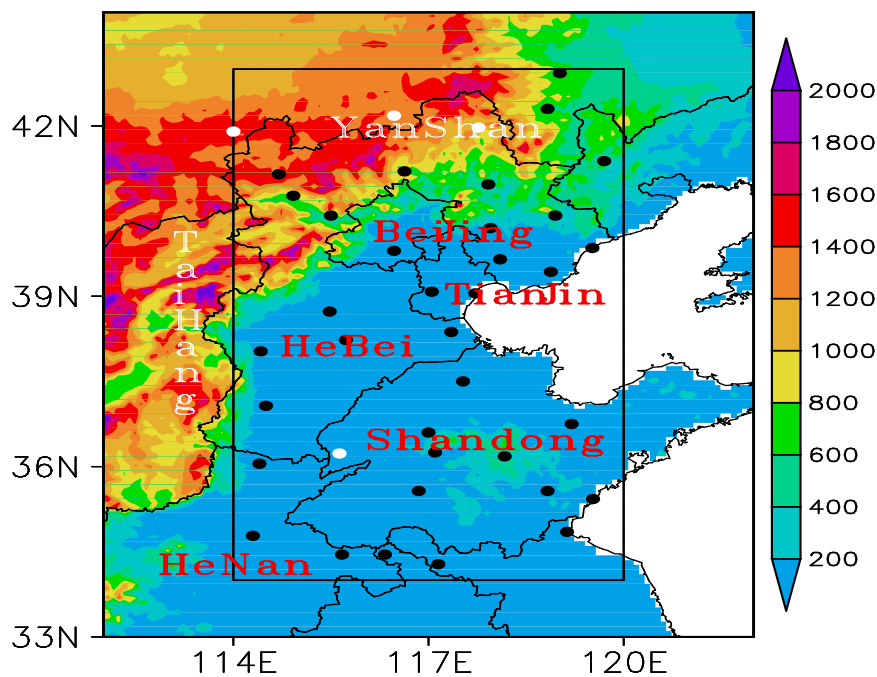


Figure 1. Topographic map (shading; unit: m) of North China and the locations of 39 NCP observation sites (Urban: black circle, Rural: white circle). The NCP area is represented by a black rectangle, and the names of provinces and mountains are written in red and white, respectively.

..... As shown in Figure 1, there were four rural stations, three of which were located near the Yan Mountains and were corresponding to less WHD. Another rural site was near the boundaries of Shandong and Henan (BSH) and also resulted in less



WHD. Figure 3b shows the WHD anomalies in 2014 with respect to 1979–2012. In addition to a few sites, a larger number of WHD occurred, especially on the BSH (rural area) and the northeast of Hebei. It is notable that WHDs in these two regions show significant increases, filling up the climatic WHD valley as shown in Figure 3a. As a result, the haze-prone area joined together, indicating that the haze pollution was more serious in this region. Actually, the fast increase of WHD in rural area was an obvious reflection of the severe haze disaster in recent years.....

**2, Correlation coefficients have been supplied by in the paper to reveal the potential effects of three patterns to WHD<sub>NCP</sub>, but necessary physical analysis of such influence has been nearly ignored by the authors.**

***Reply:***

Some necessary physical analysis has been added in section 3. The main physical mechanism was that “**climate teleconnection → local climate conditions → weaker diffusion conditions → pollutant gathered in a narrow space**”. The Figures was revised and **the order was exchanged to match the description of the physical analysis (from teleconnection to local conditions)**. The detailed analysis and revision was listed below.

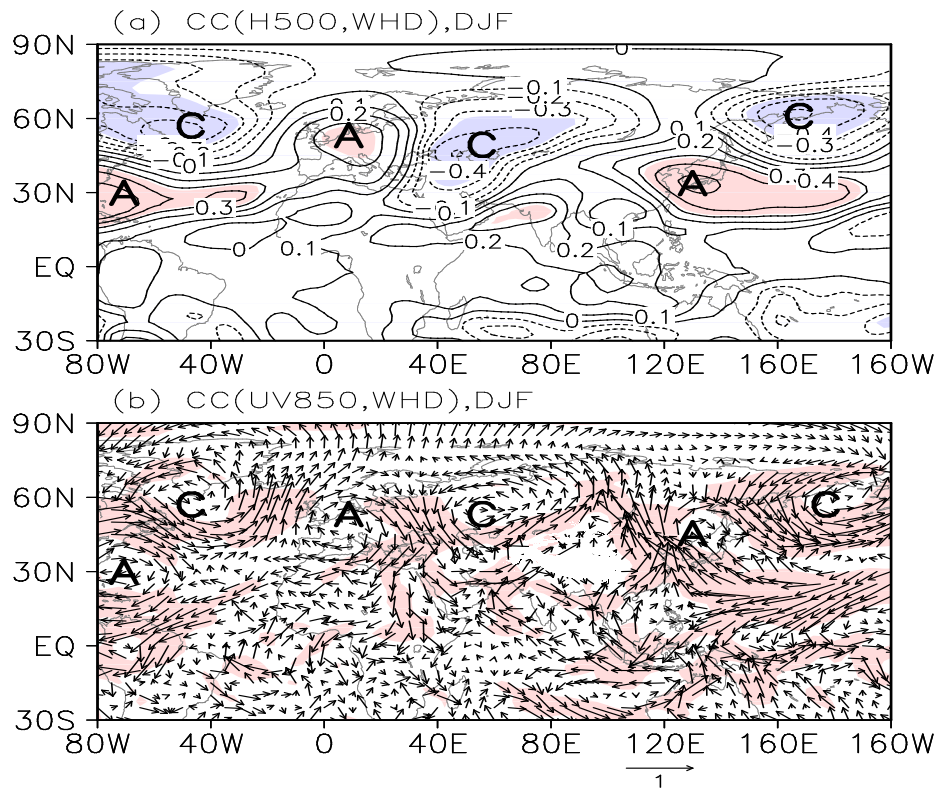
***Revision in section 3:***

.....These teleconnection patterns might contribute to WHD<sub>NCP</sub> by impacting the pivotal and local anti-cyclone anomalies (i.e., the local climate conditions) over NCP (Figure 4a–b). The deep and broad positive anomalies resulted in a thinner boundary layer by suppressing vertical movement and progressed easterly to weaken the East Asia Jet Stream (EAJS) indicating weaker meridional cold air. Near the surface, the negative SLP anomalies in the Siberia region and the Chinese Mainland and the positive SLP anomalies over the West Pacific led to a reduced pressure gradient and weakened EAWM (Figure 5a). The weaker EAWM induced the southeasterly anomalies and reduced the surface wind speed (Figure 5b), indicating weaker cold air and warmer land surface over NCP (Figure 5a). Influenced by the circulations with weaker cold air, horizontal diffusion of the atmospheric particulates

was impeded. Near NCP, the anomalous anti-cyclone also existed that illustrated weaker vertical motion. The main physical process was that the climate teleconnection patterns altered the local climate conditions, and then influenced the diffusivity of the local atmosphere. That is, when the positive pattern of EA/WR, WP and EU occurred together or partly, the anomalous anti-cyclone over NCP and Japan Sea was enhanced from surface to the middle troposphere, thus, the convection or vertical motion was confined. The southerly anomalies on the left side of this anti-cyclone weakened the cold air and wind speed. Under such local climate conditions, the vertical and horizontal diffusion of atmospheric particulates were both restricted and then the pollutant gathered in a narrow space that resulted in the occurrence of haze.

In winter 2014, many extreme climatic events occurred, such as severe drought and high temperatures in NCP (Wang et al. 2015). Corresponding external forcings should be observed as the background of these extreme synoptic and climatic events, which might persistently impacted the atmospheric circulations and led to an irregular distribution of teleconnection patterns in winter. It should be noted that EA/WR pattern in winter 2014 was distributed slightly westwards and broadly. Nevertheless, the three eastern centers of EA/WR, WP and EU patterns could be recognized (Figure 4c). The linkage system of these three teleconnection patterns was enhanced and modulated the local climate conditions. The NCP area was influenced by the anomalous high resulting in lower PBLH (Figure 6). The southerly at the high latitudes deadened the cold air from its main source, so the atmospheric matters gathered easily. Near the surface, the negative SLP anomalies occupied the whole Asian continent and Japan Sea that weakened the continental cold high and stimulated significant southerly anomalies to the north of 50°N with the weaker Aleutian low. The weaker EAWM circulations near the surface blocked the cold air from high latitudes and resulted in warmer surface (Wang et al. 2015). There were positive SLP anomalies over South China Sea and East China Sea that induced southerly and smaller surface wind speed over the coastal area in the east of China (Figure 5c—d).

The diffusivity of atmosphere over the NCP was limited, so the high pollutant emissions were concentrated in a narrow space and severe haze events occurred easily. Large scale circulations, such as the negative phase of EA/WR and WP, were quite clear in 2010 (Figure 5d). Near the surface, the anomalous circulations were distributed similarly but almost opposite, i.e., the stronger continental cold high and oceanic low (Figure 5e), the northerly and stronger surface wind over NCP (Figure 5f) , and the higher PBLH (Figure 6). The atmospheric diffusivity was heightened by the stronger cold air and vertical movement. This observation further supports the speculation that the anomalous EA/WR and WP patterns contributed to significant changes in  $WHD_{NCP}$  by altering the local climate conditions. The anomalies of the EU pattern in winter 2010 were not as significant as those in 2014. As shown by Table 1, the relationship between  $WHD_{NCP}$  and the EU index weakened after detrending, illustrating that the correlation was much weaker than the other two patterns.....



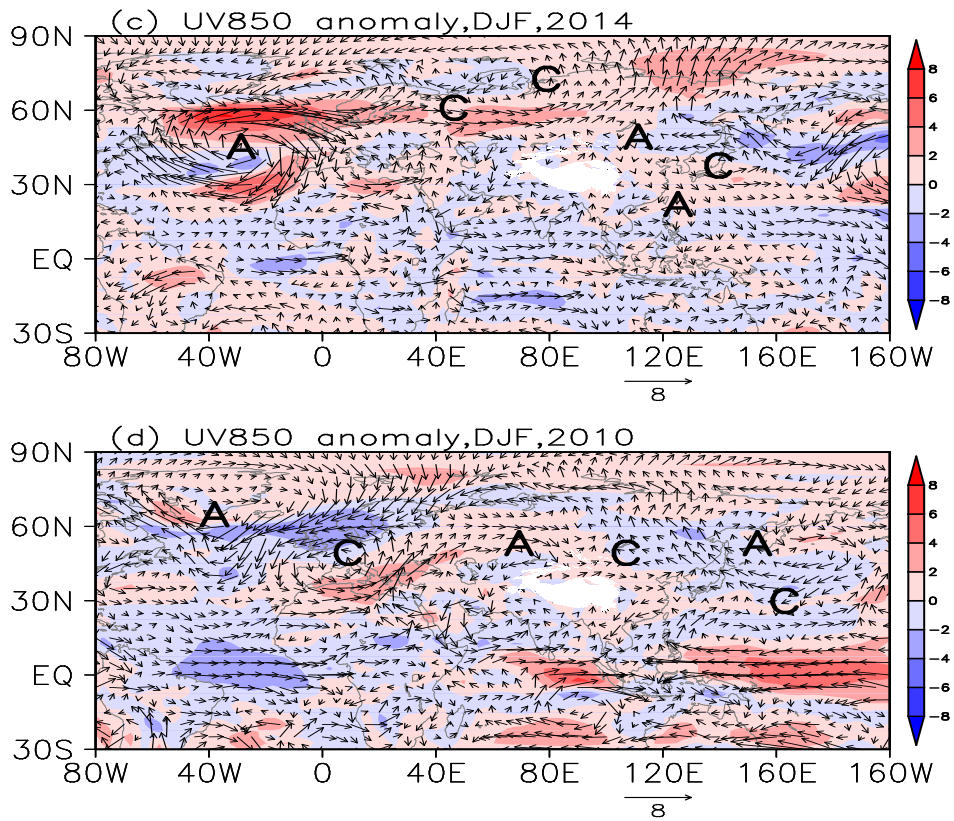
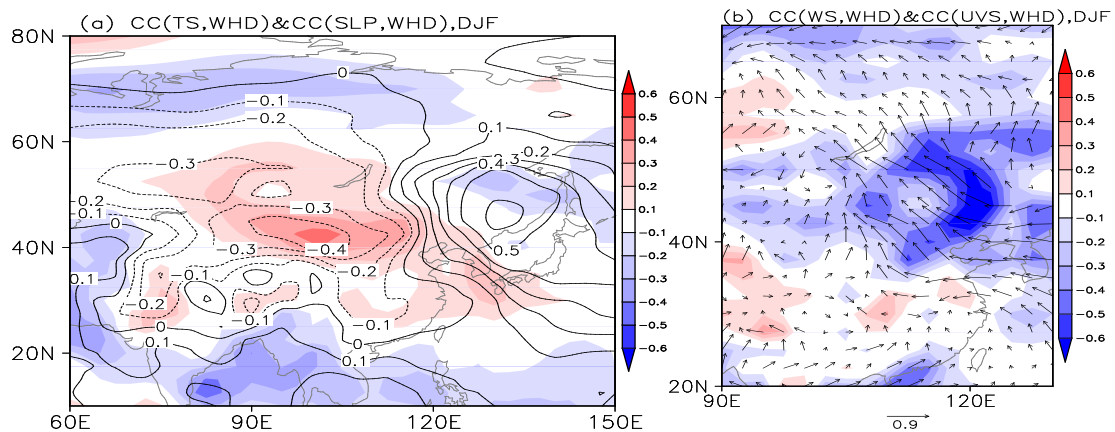


Figure 4. Correlation coefficients between  $WHD_{NCP}$  and winter H500 (a) / UV850 (b) from 1979 to 2012. The linear trend was removed, and shade indicates that CC exceeds the 95% confidence level. UV850 (arrow) and speed (shade) anomalies in winter 2014 (c) and 2010 (d). A and C represent anti-cyclone and cyclone, respectively.



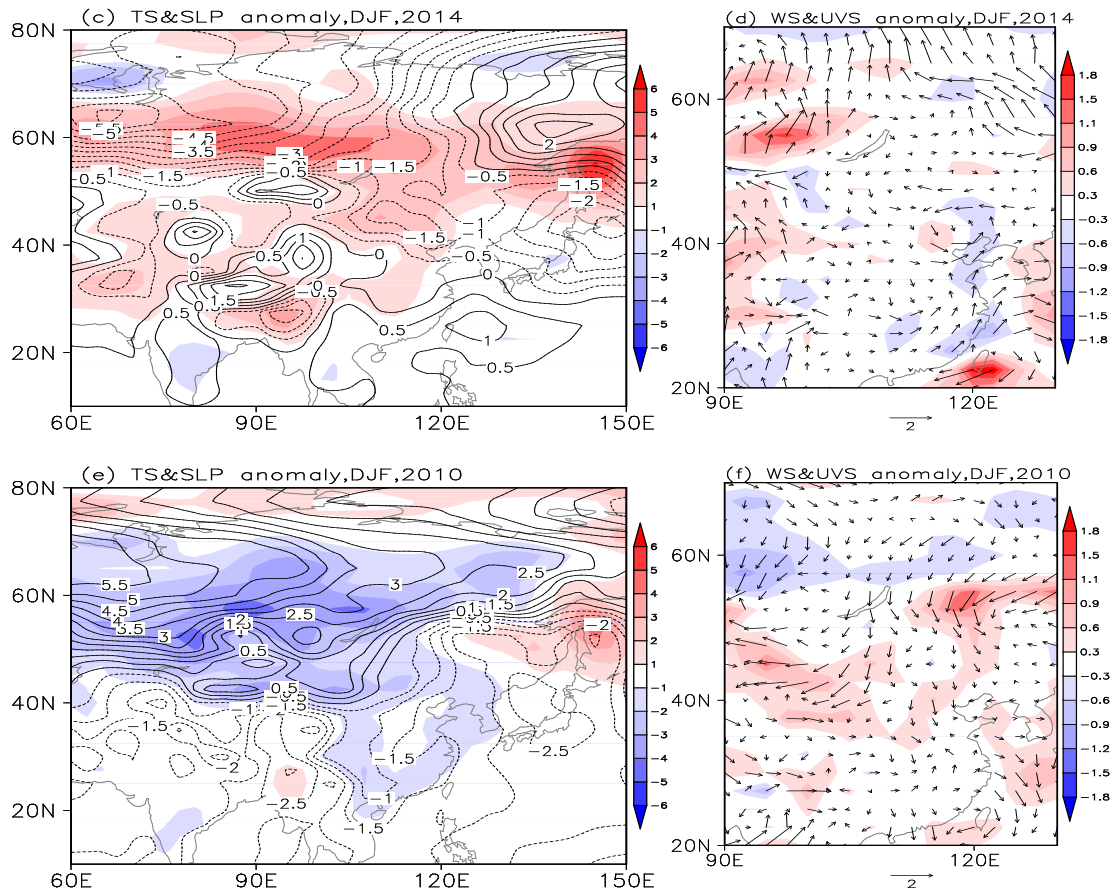


Figure 5. Correlation coefficients between  $WHD_{NCP}$  and winter circulations from 1979 to 2012 with linear trend was removed (a, b), and circulation anomalies in 2014 (c, d) and 2010 (e, f). The circulations in (a, c, e) are TS (shade) and SLP (contour) and those in (c, d, f) are surface wind speed (shade) and wind vector (arrow).

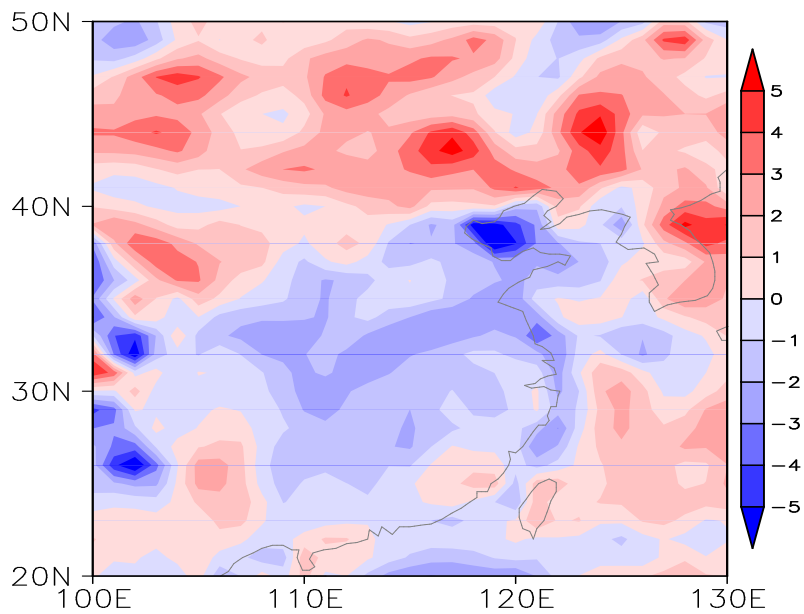


Figure 6. The difference of winter PBLH between 2014 and 2010

3, Concentration of PM<sub>2.5</sub> reached its maximum in 2013, therefore the annual changes of emission should play an very important role in the haze days in recent years, but the author failed to arrange enough discussion and analysis about the emission change.

*Reply:*

To enhance our perspective, the title has been changed to “Understanding Severe Winter Haze Events in the North China Plain in 2014: Roles of Climate Anomalies”. The main purpose of this study was to discuss the roles of climate conditions. The impact of emissions was written in the “Introduction” and “Discussion”.

No doubt that the long-term increase of pollutant emission is the fundamental factor for the haze pollution enhancement in recent years. However, so far, **there is no evidence that the emissions were more in 2014 than in 2010**. Furthermore, the PM<sub>2.5</sub> concentration of a global atmospheric watch station (Shangdianzi) and an urban station (Baolian) were **almost equal** in winter 2010 and 2014. By our current and some previous analysis, we found that **the climate factor played key roles in the formation of the heavy pollution case like 2014**.

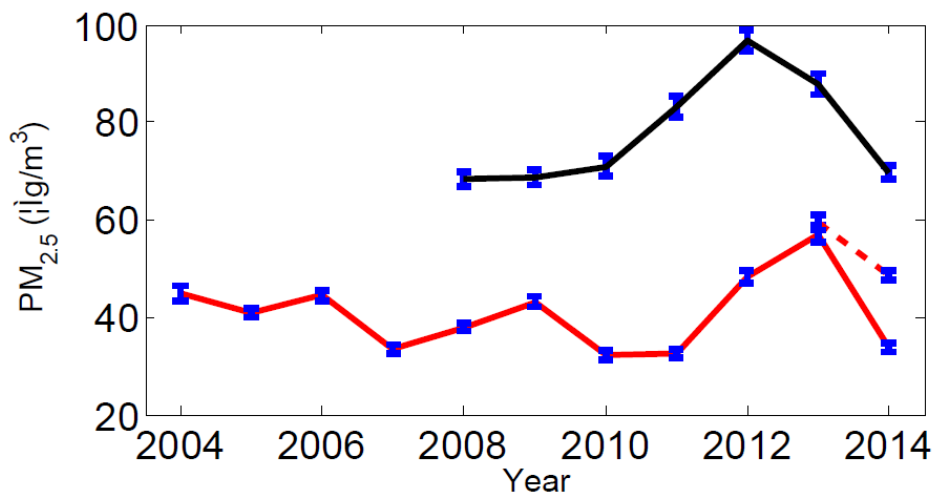


Figure 11. Mean mass concentration of PM<sub>2.5</sub> in winter at Shangdianzi (red; measured by the TOEM (solid) and  $\beta$ -ray (red dash) method) and Baolian (black) Station. The error bar represents one standard error among the different measured hours.

The anthropogenic emissions were the fundamental driver and mostly impacted the long-term trend of the haze pollution. To some extent, the energy consumption

varied continuously and linearly in eastern China and **the socio-economic components of WHD<sub>NCP</sub> could be removed primitively by detrending**, and then the interannual variability of haze pollution should be mainly the result of climatic anomalies.

The case studies of 2013 enhanced that the pollutant emission is the fundamental factor and highlighted the roles of anthropogenic influence. **The concentration in winter 2013 increased abruptly up to nearly twice that in 2010 and 2014 and was the highest in the observation history that broke down our assumption. Even the anomalous circulations were not benefit enough for haze occurrence, the joint effect of highest pollution emissions and climate conditions could result in the serious haze event.** A brief summary of the impacts of these factors on WHD<sub>NCP</sub> is offered in Table 2.

**Table 2. Summary of the various influence factors for WHD<sub>NCP</sub>. The “+++” indicates “more important”; “++” indicates “important”, “+” indicates “less important”, and blank indicates “not important”.**

<i>Factors</i>	<i>2010</i>	<i>2013</i>	<i>2014</i>
<b>PM<sub>2.5</sub> concentration</b>	++	+++	++
Local surface wind speed	++	++	++
Local PBLH	++	++	++
EA/WR	++	++	++
WP	++		++
EU			++
Pre-autumn ASI	++		++
Winter TS	++		++
ON Pacific SSTA	+	++	++
Pre-autumn TS	++		++
SON Atlantic SSTA		++	

**Revision:**

In the Introduction section:

There is no doubt that the anthropogenic emissions were the fundamental cause for the long-term variation of haze days in eastern China (Wang et al. 2013). The enormous energy consumption supplied enough particulates, so the atmosphere tended to reach saturation. Thus, the impact of meteorological conditions is highlighted and the climate conditions are also vital contributors to the interannual

variation of haze (Liao et al. 2014). For example, the joint effect of fast increase of total energy consumption, rapid decline of Arctic sea ice extent and reduced precipitation and surface winds intensified the haze pollution in central North China after 2000 (Wang et al. 2016).....

In the discussion section:

.....Except for a few sites, haze pollution over NCP in winter 2014 was the severest in the past 30 years. On the BSH area and the northeast of Hebei, WHD increased significantly and invaded into the rural area, illustrating a joint and broad severe haze-prone region. **The PM<sub>2.5</sub> concentration at a GAWS and an urban site were almost equal in winter 2010 and 2014, so there was no evidence that the emissions were more in 2014 than 2010. The climate conditions played key roles in the formation of heavy haze pollution case in 2014.** On the lower and middle troposphere, the positive phases of EA/WR, WP and EU patterns modulated the local anti-cyclone anomalies over North China. The anti-cyclone anomalies over East Asia not only resulted in stable atmospheric stratification and a thinner boundary layer but also led to a southeasterly anomaly that weakened the cold air but enhanced the moisture transport. The atmospheric matters would accumulate easily both on the vertical and horizontal direction. In winter 2014, the teleconnection patterns, such as EA/WR, EU and WP, combined to alter the local climate conditions to contribute to the extreme haze case. SVD analyses indicated that the pre-autumn ASI anomalies of the Eastern Hemisphere and the warmer winter surface of Eurasia could have induced or intensified the responses in the atmosphere, resembling a positive EA/WR pattern. These two external forcings, together with the SSTA in Pacific (i.e., cooler in the northwest Pacific and warmer in the central-east Pacific and Alaska Gulf) might stimulate or enhance positive EU-like patterns. In autumn 2014, the “southwest to northeast” anomalous TS belts were other factors that efficiently intensified the haze pollutions, which resulted in a positive phase of the WP pattern. The case of 2010, with the least WHD<sub>NCP</sub>, was diagnosed as an opposite case, which further supports the speculation that the anomalous EA/WR and WR patterns and associated external forcings have a significant impact on WHD<sub>NCP</sub>. Additionally, as pointed out by Wang



et al. (2015), the Asian high temperature and drought from summer in 2014 was an extreme climate event. Our studies proved that this previous extreme climate event possibly contributed to the serious haze event in the following winter.

The rapid increase of  $WHD_{NCP}$  began in January 2013, and in winter 2013 and 2014,  $WHD_{NCP}$  was significantly greater than before. The  $WHD_{NCP}$  in 2013 and 2014 was greater than 50 days and almost equal to each other (Figure 2). Therefore, the causes of serious haze in 2013 should also be discussed. The anomalous circulations in winter 2013 were not as favorable for haze as those in 2014. The EA/WR pattern was well organized and showed a positive phase that was distributed slightly eastwards (Figure S6). Influenced by the upper EA/WR pattern, the surface wind speed was slower and the PBLH was lower, illustrating the horizontal and vertical diffusivity of the atmosphere was weaker (Figure S7). The EU and WP patterns were unclear. The source region of EU even showed characteristics of a negative phase. According to the 2010 and 2014 case studies, the preceding and simultaneous external forcings could have impacted the  $WHD_{NCP}$ . In contrast, the pre-autumn ASI and TS and winter TS in 2013 did not show features similar to those in 2014 (Figure S8). The pre-autumn Pacific SSTA, which was slightly negative in the northwest Pacific and positive in the Alaska Gulf and central-east Pacific, could have stimulated positive anomalies over NCP and weakened the East Asia trough. Thus, it can be observed that, among many external reasons for the extreme haze in 2014, only the pre-autumn Pacific SSTA was distributed similarly in 2013. The EA/WR Rossby wave train was the prominent circulation contributing to  $WHD_{NCP}$  in 2013, with a source located over the central-north Atlantic. We speculate that the air-sea interaction over north Atlantic excited the EA/WR pattern in the atmosphere and influenced  $WHD_{NCP}$  remotely. The correlation coefficients between the EA/WR index and the pre-autumn SST in Atlantic were calculated and were significantly positive to the south of Greenland (Figure S9b). When the SSTA to the south of Greenland was positive, the responses similar to EA/WR occurred in the atmosphere. The pre-autumn SSTA in the Atlantic in 2013 was similar to that shown in Figure S9b and might have

remotely impacted  $WHD_{NCP}$  via the EA/WR pattern. It should be noted that the SSTA of the key region in the Atlantic was negative and had an adverse effect on  $WHD_{NCP}$  in 2014.

From the point of facilitating a larger amount of  $WHD_{NCP}$ , the associated circulations and external forcings in 2013 were different from that in 2014, but the serious situations of haze were almost the same. **In our study, we assumed that the energy consumption linearly increased in the recent years. On such hypothesis, the human activities mainly impacted the long-term trend of  $WHD_{NCP}$ . After removal of the linear trend, the interannual variability of haze pollution should be mainly the result of climatic anomalies.** The Shangdianzi site is the only GAWS in North China and was chosen to reflect the natural or background situation of the atmosphere. The mean mass concentrations of  $PM_{2.5}$  in winter from 2004 to 2014 are plotted in Figure 11. **The concentration in winter 2013 increased abruptly up to nearly twice that in 2010 and 2014 and was the highest in the observation history that broke down our assumption.** Furthermore, the  $PM_{2.5}$  concentration of an urban site, Blaolian station, was also much higher than 2010 and 2014. **Even the anomalous circulations were not benefit enough for haze occurrence, the joint effect of highest pollution emissions and climate conditions could result in the serious haze event.** Documented by these three case studies, the influences of the highest concentrations of  $PM_{2.5}$  were the fundamental cause, and the associated with atmospheric anomalies and external forcings played key roles in the severe haze pollution. In this study, we focused on the roles of climate conditions and did not discuss the impact of human activities deeply that should be researched in the future work. To separate the contributions quantitatively by numerical models or advanced statistical approaches would be a meaningful task that was helpful to the interpretation of mechanism and the seasonal prediction (Yin et al. 2016b). In the case studies, 2010 and 2014 exhibited approximately equal  $PM_{2.5}$  concentrations of the background atmosphere, but the associated circulations and external forcings in 2010 were still slightly different from those in 2014. It is possible that not all of the above factors

might be found in a specific case study, i.e., a few of these effective factors played the essential roles and led to the characteristics of that case. A brief summary of the impacts of these factors on  $WHD_{NCP}$  is offered in Table 2.....

**4, Line 20: EA/WA should be EA/WR**

***Reply:***

The error has been corrected.

***Revision:***

.....in 2010 further supports the mechanism of how EA/WR and WP patterns and associated external factors impact.....

**5, Line 36: What's the specific criterion of "static stability"?**

***Reply:***

The "static stability" was the ability of a fluid at rest to become turbulent or laminar due to the effects of buoyancy. The static stability of the atmosphere could indicate the vertical motion potential (or the intensity of convection) that was important for weather and pollution forecast.

Throughout the paper, the term "static stability" was only used once and in the introduction. Thus, we decided to correct it to a clearer and simpler expression "stable atmosphere".

***Revision:***

SWP-SST weakened EAWM circulation, leading to a favorable environment for haze with stable atmosphere and potential for hygroscopic growth (Yin et al. 2016).

**6, Line 69-83: What's the role of Fig. 2 in such an analysis of large scale analysis for  $WHD_{NCP}$  in 2014 ?**

***Reply:***

As we know, haze is a multidisciplinary phenomenon that can be represented by visibility and humidity in meteorology, and by the concentration of the atmospheric composition in environmental science. The older Figure 2 was plotted to demonstrate

the representation of haze data reconstructed primarily by visibility. After comparison, we confirmed that **the derived haze datasets not only agreed with the meteorological standard but also satisfactorily represented the concentration of the atmospheric composition.**

Following the reviewers advice, we putted this Figure into the supplementary material (i.e., Figure S1).

***Revision:***

Figure S1. Visibility of Beijing (green) and atmospheric.....

**7, Line 109: two “that”.**

***Reply:***

The error has been corrected.

***Revision:***

It is notable that WHDs in these two regions show significant increases, filling up the climatic WHD valley as shown in Figure 3a.

## **Reply letter to the anonymous Referee #2**

Received and published: 14 October 2016

In this work, the authors discussed the possible mechanisms of the severe haze pollution over the North China Plain in winter. Three teleconnection patterns (EA/WR, WP and EU) might have led to stable meteorological conditions that contributed to severe haze events over the North-Central North China Plain in 2014. Using SVD analysis, several external forcings were pointed out to have enhanced certain teleconnection patterns. This paper highlights the links between external forcings, teleconnection patterns and WHDs, but more discussions in detail were still needed in this paper:

**1. 39 NCP stations were used to reconstruct the climatic WHDs, significant spatial variation of WHDs could be observed in Figure 4(a). Only four rural stations were selected to represent urban haze. The authors didn't introduce the locations of the four stations.**

### ***Reply:***

**Our motivation is to address the haze pollution in large area, including both the urban and rural regions.** The reason for that only 4 rural sites were selected was the limited quality and temporal range of the rural measurements. However, reminded by the reviewer, **the Figure 1 was revised to introduce the location of the rural sites and some new features were revealed.** From the Figure 1 and 2a, we can see that the areas with less WHD were near the rural stations. Actually, the fast increase of WHD in rural area was an obvious reflection of the severe haze disaster in recent years. In other words, the coverage of haze invaded into the rural region in 2014.

### ***Revision:***

.....Due to the quality and temporal range of the data, only four rural stations were qualified and selected (white circles in Figure 1). ~~and the datasets tended to represent the characteristics of urban haze.....~~

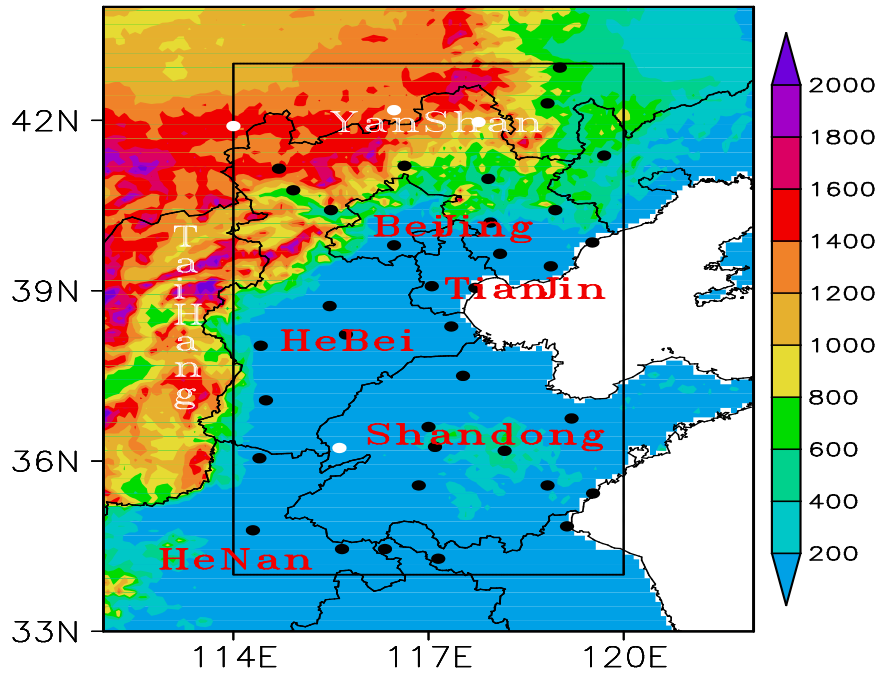


Figure 1. Topographic map (shading; unit: m) of North China and the locations of 39 NCP observation sites (Urban: black circle, Rural: white circle). The NCP area is represented by a black rectangle, and the names of provinces and mountains are written in red and white, respectively.

.....As shown in Figure 1, there were four rural stations, three of which were located near the Yan Mountains and were corresponding to less WHD. Another rural site was near the boundaries of Shandong and Henan (BSH) and also resulted in less WHD. Figure 3b shows the WHD anomalies in 2014 with respect to 1979–2012. In addition to a few sites, a larger number of WHD occurred, especially on the BSH (rural area) and the northeast of Hebei. It is notable that WHDs in these two regions show significant increases, filling up the climatic WHD valley as shown in Figure 3a. As a result, the haze-prone area joined together, indicating that the haze pollution was more serious in this region. Actually, the fast increase of WHD in rural area was an obvious reflection of the severe haze disaster in recent years.....

**2. During the period from 1979 to 2012, the negative SLP anomaly in the Siberia region and the positive SLP anomaly over West Pacific led to weakened EAWM inducing the southeasterly anomaly (Figure 5 (a) and (c)), which was favorable for haze events. But in 2014, anomalies of meteorological fields (Figure 5 (b) and (d)) for WHDs in the NCP region were different from those in 1979-2012.**

Although the surface temperature was higher than average over the Asian continent, the surface wind fields over NCP region didn't show favorable conditions for WHDs. As anthropogenic emissions could also influence air quality, meteorological conditions might not be the main cause of WHDs in 2014.

*Reply:*

(1) So far, **there is no evidence that the emissions were more in 2014 than 2010**. Furthermore, the  $PM_{2.5}$  concentration of a global atmospheric watch station (Shangdianzi) and an urban station (Baolian) were **almost the same** in winter 2010 and 2014. By our current and some previous analysis, we found that **the climate factor played key roles in the formation of the heavy pollution case like 2014**.

The anthropogenic emissions were the fundamental driver and mostly impacted the long-term trend of the haze pollution. To some extent, the energy consumption varied continuously and linearly in eastern China and **the socio-economic components of  $WHD_{NCP}$  could be removed primitively by detrending**, and then the interannual variability of haze pollution should be mainly the result of climatic anomalies.

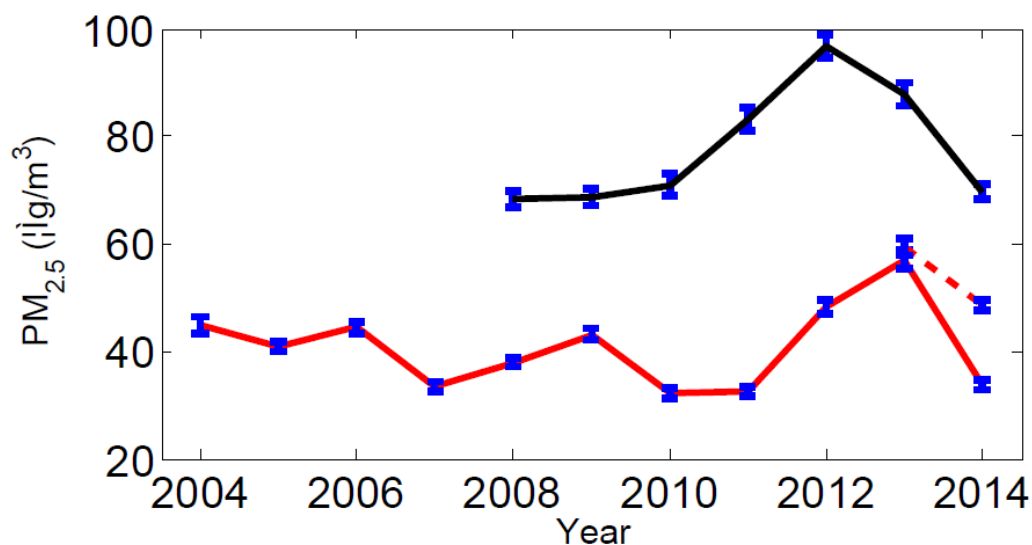


Figure 11. Mean mass concentration of  $PM_{2.5}$  in winter at Shangdianzi (red; measured by the TOEM (solid) and  $\beta$ -ray (red dash) method) and Baolian (black) Station. The error bar represents one standard error among the different measured hours.

To enhance our perspective, the title has been changed to “Understanding Severe Winter Haze Events in the North China Plain in 2014: Roles of Climate Anomalies”. The main purpose of this study was to discuss the roles of climate anomalies and the impact of emissions is discussed in the “Introduction” and “Discussion”.

(2) In the discussion section, we pointed out “the associated circulations and external forcings in 2010 were still slightly different from those in 2014. It is possible that **not all of the above factors might be found in a specific case study, i.e., a few of these factors played the essential roles and led to the characteristics of that case.** A brief summary of the impacts of these factors on WHD<sub>NCP</sub> is offered in Table 2”. The Table 2 was improved to include all of the possible factors. In summary, the local climate conditions, (i.e., weaker surface wind speed and lower PBLH), the teleconnection patterns and the external forcings were benefit for the occurrence of the haze extreme in 2014.

**Table 2. Summary of the various influence factors for WHD<sub>NCP</sub>. The “+++” indicates “more important”; “++” indicates “important”, “+” indicates “less important” , and blank indicates “not important”.**

<i>Factors</i>	<i>2010</i>	<i>2013</i>	<i>2014</i>
PM <sub>2.5</sub> concentration	++	+++	++
Local surface wind speed	++	++	++
Local PBLH	++	++	++
EA/WR	++	++	++
WP	++		++
EU			++
Pre-autumn ASI	++		++
Winter TS	++		++
ON Pacific SSTA	+	++	++
Pre-autumn TS	++		++

To enhance our analysis of 2014 case, the anomalies of meteorological fields were re-plotted and the composite of PBLH was supplemented. ① For the **horizontal diffusion**: The main argument was that the weaker EAWM pattern could intensify the haze pollution in the NCP. Except the SLP anomalies over Northeast



China and Japan Sea, the pressure field was also similar with the climatic correlation. Furthermore, the surface wind anomalies at the high latitude blocked the cold air from their source and there were southerly to the south of 40°N that occupied most of our research area. Unfortunately, the isolated northerly could be found to the north of 40°N. That is, the large scale EAWM pattern and most of the synoptic scale circulations were benefit for the large number of WHD<sub>NCP</sub> in winter 2014. ② **For the vertical diffusion:** The composite of PBLH was supplemented as Figure 6. The PBLH was a good indicator for air pollution, especially for the vertical diffusivity. The winter PBLH in 2014 was much lower than that in 2010, so the vertical diffusivity was worse in 2014 resulting in more haze days.

***Revisions to the impact of human activities were showed in the replies to Q4:***

***Revision to the meteorological conditions in 2014:***

.....Nevertheless, the three eastern centers of EA/WR, WP and EU patterns could be recognized (Figure 4c). The linkage anti-cyclone of these three teleconnection patterns was enhanced and modulated the local climate conditions. The NCP area was influenced by the anomalous high resulting in lower PBLH (Figure 6). The southerly at the high latitudes deadened the cold air from its main source, so the atmospheric matters gathered easily. Near the surface, the negative SLP anomalies occupied the whole Asian continent and Japan Sea that weakened the continental cold high and stimulated significant southerly anomalies to the north of 50°N with the weaker Aleutian low. The weaker EAWM circulations near the surface blocked the cold air from high latitudes and resulted in warmer surface (Wang et al. 2015). There were positive SLP anomalies over South China Sea and East China Sea that induced southerly and smaller surface wind speed over the coastal area in the east of China (Figure 5c—d). The diffusivity of atmosphere over the NCP was limited, so the high pollutant emissions were concentrated in a narrow space and severe haze events occurred easily.....

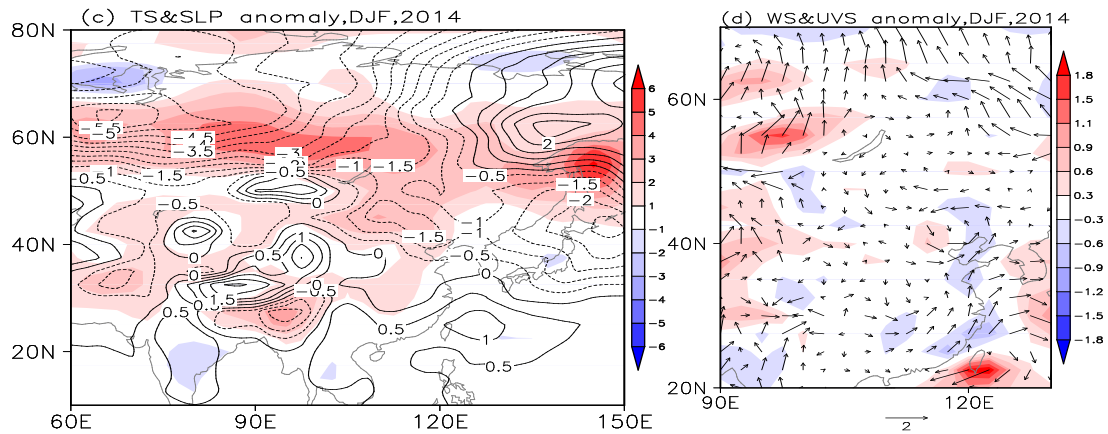


**Figure 5. Correlation coefficients between  $WHD_{NCP}$  and winter circulations from 1979 to 2012 with linear trend was removed (a, b), and circulation anomalies in 2014 (c, d) and 2010 (e, f). The circulations in (a, c, e) are TS (shade) and SLP (contour) and those in (c, d, f) are surface wind speed (shade) and wind vector (arrow).**

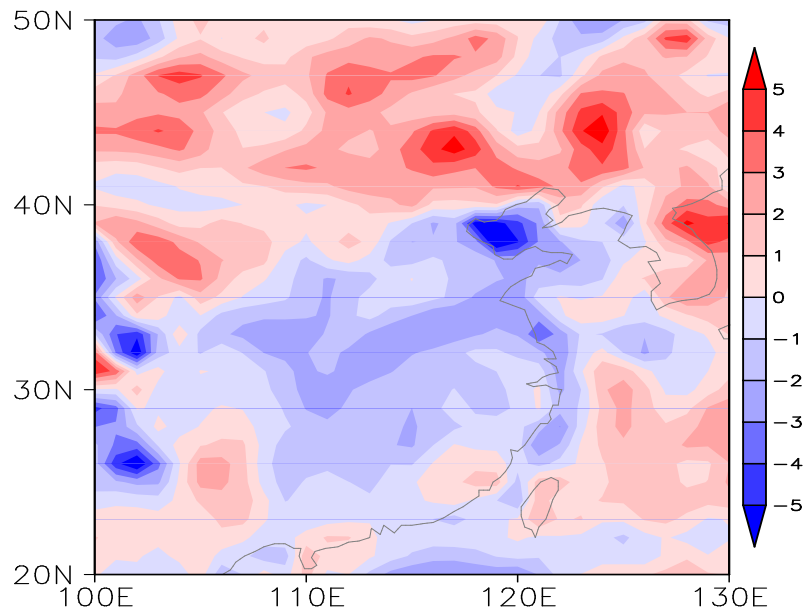


**Figure 6. The difference of winter PBLH between 2014 and 2010**

**3. Two extreme haze phenomenon were discussed in this work. Teleconnection patterns in 2010 and 2014 were different, but over the NCP region, anomalous circulations of wind fields in 2010 were similar with those in 2014. And the authors didn't discuss the regional meteorological conditions over NCP region in detail in 2010. Thus, in order to prove the importance of meteorological conditions on these two haze events the authors need to provide more evidences to support their arguments.**

**Reply:**

The regional meteorological conditions in 2010 were supplemented as Figure 5e—f and 6 that showed similar but opposite features. As reply to Q2, we discussed that it is possible that not all of the above factors might be found in a specific case study, i.e., only a few of these effective factors **played the essential roles and** led to the characteristics of that case. A brief summary of the impacts of these factors on WHD<sub>NCP</sub> is offered in Table 2”. ① **For 2010**, the local climate conditions (i.e., weaker surface wind speed and lower PBLH), most of the teleconnections (except the EU) and the external forcings played positive roles to less haze days. ② **For 2014**, In the local climate conditions, (i.e., weaker surface wind speed and lower PBLH), the teleconnection patterns and the external forcings were benefit for the occurrence of the haze extreme in 2014.

**Table 2. Summary of the various influence factors for WHD<sub>NCP</sub>. The “+++” indicates “more important”; “++” indicates “important”, “+” indicates “less important” , and blank indicates “not important”.**

<i>Factors</i>	<i>2010</i>	<i>2013</i>	<i>2014</i>
PM <sub>2.5</sub> concentration	++	+++	++
Local surface wind speed	++	++	++
Local PBLH	++	++	++
EA/WR	++	++	++
WP	++		++
EU			++
Pre-autumn ASI	++		++
Winter TS	++		++
ON Pacific SSTA	+	++	++
Pre-autumn TS	++		++

**Revision:**

.....Large scale circulations, such as the negative phase of EA/WR and WP, were quite clear in 2010 (Figure 4d). Near the surface, the anomalous circulations were distributed similarly but almost opposite, i.e., the stronger continental cold high and oceanic low (Figure 5e), the northerly and stronger surface wind over NCP

(Figure 5f), and the higher PBLH (Figure 6). The atmospheric diffusivity was heightened by the stronger cold air and vertical movement.....

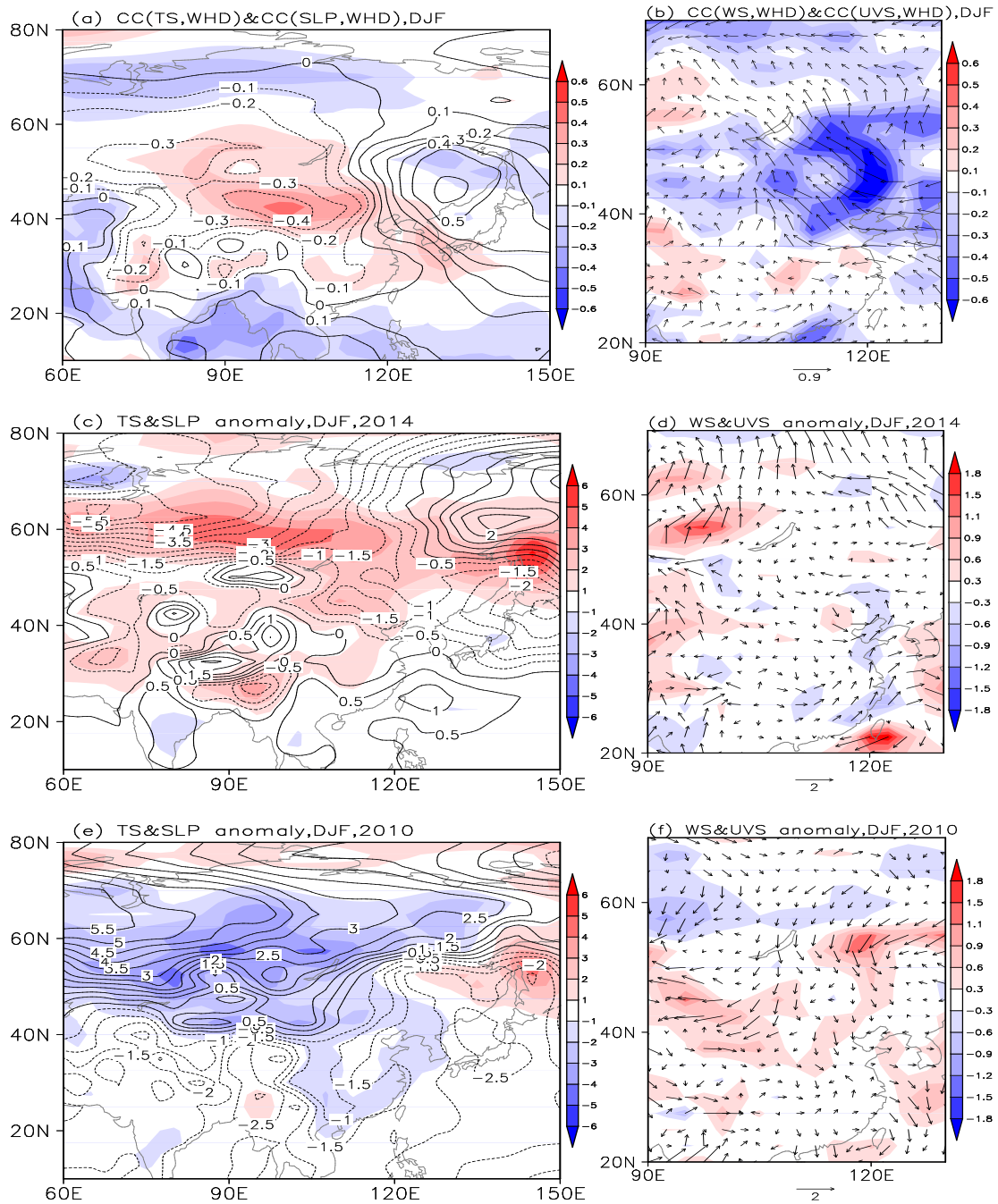


**Figure 5. Correlation coefficients between WHD<sub>NCP</sub> and winter circulations from 1979 to 2012 with linear trend was removed (a, b), and circulation anomalies in 2014 (c, d) and 2010 (e, f). The circulations in (a, c, e) are TS (shade) and SLP (contour) and those in (c, d, f) are surface wind speed (shade) and wind vector (arrow).**

**4. The authors concluded that anomalous circulations in winter 2013 were not as**

**favorable for haze conditions as those in 2014. But the number of WHDs in 2013 was as large as that in 2014. Does it mean that the influence of anthropogenic influence was more significant in 2013 than in 2014? How could the authors eliminate the influence of anthropogenic influence?**

*Reply:*

(1) No doubt that the long-term increase of pollutant emission is the fundamental factor for the haze pollution enhancement in recent years. **However, so far, there is no evidence that the emissions were more in 2014 than in 2010.** By our current and some previous analysis, we found that the climate factor played key roles in the formation of the heavy pollution case like 2014. After removal of the linear trend, the interannual variability of haze pollution should be mainly the result of climatic anomalies. **Thus, we removed the socio-economic components of  $WHD_{NCP}$  primitively by detrending.** To enhance our perspective, the title has been changed to “Understanding Severe Winter Haze Events in the North China Plain in 2014: Roles of Climate Anomalies”.

(2) The impact of emissions was discussed in the “Introduction” and “Discussion”. **We also talked about the anthropogenic influence to the 2013 case. The concentration in winter 2013 increased abruptly up to nearly twice that in 2010 and 2014 and was the highest in the observation history that broke down our assumption.** Even the anomalous circulations were not benefit enough for haze occurrence, the joint effect of highest pollution emissions and climate conditions could result in the serious haze event.

In the former version, we concluded that the anomalous in 2013 was not favorable as 2014 curtly. Now, we decided to cancel this conclusion and discuss the comparison more objectively in the last section to show the difference between 2013 and 2014.

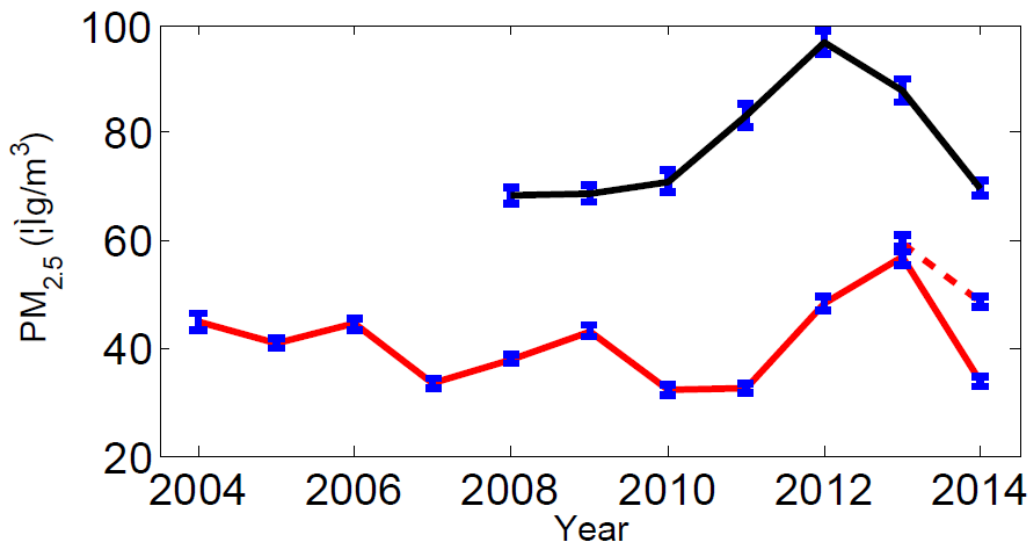


Figure 11. Mean mass concentration of PM<sub>2.5</sub> in winter at Shangdianzi (red; measured by the TOEM (solid) and β-ray (red dash) method) and Baolian (black) Station. The error bar represents one standard error among the different measured hours.

**Revision:**

In the Introduction section:

There is no doubt that the anthropogenic emissions were the fundamental cause for the long-term variation of haze days in eastern China (Wang et al. 2013). The enormous energy consumption supplied enough particulates, so the atmosphere tended to reach saturation. Thus, the impact of meteorological conditions is highlighted and the climate conditions are also vital contributors to the interannual variation of haze (Liao et al. 2014). For example, the joint effect of fast increase of total energy consumption, rapid decline of Arctic sea ice extent and reduced precipitation and surface winds intensified the haze pollution in central North China after 2000 (Wang et al. 2016).....

In the discussion section:

.....Except for a few sites, haze pollution over NCP in winter 2014 was the severest in the past 30 years. On the BSH area and the northeast of Hebei, WHD increased significantly and invaded into the rural area, illustrating a joint and broad severe haze-prone region. **The PM<sub>2.5</sub> concentration at a GAWS and an urban site were almost equal in winter 2010 and 2014, so there was no evidence that the**

**emissions were more in 2014 than 2010. The climate conditions played key roles in the formation of heavy haze pollution case in 2014.** On the lower and middle troposphere, the positive phases of EA/WR, WP and EU patterns modulated the local anti-cyclone anomalies over North China. The anti-cyclone anomalies over East Asia not only resulted in stable atmospheric stratification and a thinner boundary layer but also led to a southeasterly anomaly that weakened the cold air but enhanced the moisture transport. The atmospheric matters would accumulate easily both on the vertical and horizontal direction. In winter 2014, the teleconnection patterns, such as EA/WR, EU and WP, combined to alter the local climate conditions to contribute to the extreme haze case. SVD analyses indicated that the pre-autumn ASI anomalies of the Eastern Hemisphere and the warmer winter surface of Eurasia could have induced or intensified the responses in the atmosphere, resembling a positive EA/WR pattern. These two external forcings, together with the SSTA in Pacific (i.e., cooler in the northwest Pacific and warmer in the central-east Pacific and Alaska Gulf) might stimulate or enhance positive EU-like patterns. In autumn 2014, the “southwest to northeast” anomalous TS belts were other factors that efficiently intensified the haze pollutions, which resulted in a positive phase of the WP pattern. The case of 2010, with the least  $WHD_{NCP}$ , was diagnosed as an opposite case, which further supports the speculation that the anomalous EA/WR and WR patterns and associated external forcings have a significant impact on  $WHD_{NCP}$ . Additionally, as pointed out by Wang et al. (2015), the Asian high temperature and drought from summer in 2014 was an extreme climate event. Our studies proved that this previous extreme climate event possibly contributed to the serious haze event in the following winter.

The rapid increase of  $WHD_{NCP}$  began in January 2013, and in winter 2013 and 2014,  $WHD_{NCP}$  was significantly greater than before. The  $WHD_{NCP}$  in 2013 and 2014 was greater than 50 days and almost equal to each other (Figure 2). Therefore, the causes of serious haze in 2013 should also be discussed. The anomalous circulations in winter 2013 were not as favorable for haze as those in 2014. The EA/WR pattern was well organized and showed a positive phase that was distributed slightly

eastwards (Figure S6). Influenced by the upper EA/WR pattern, the surface wind speed was slower and the PBLH was lower, illustrating the horizontal and vertical diffusivity of the atmosphere was weaker (Figure S7). The EU and WP patterns were unclear. The source region of EU even showed characteristics of a negative phase. According to the 2010 and 2014 case studies, the preceding and simultaneous external forcings could have impacted the  $WHD_{NCP}$ . In contrast, the pre-autumn ASI and TS and winter TS in 2013 did not show features similar to those in 2014 (Figure S8). The pre-autumn Pacific SSTA, which was slightly negative in the northwest Pacific and positive in the Alaska Gulf and central-east Pacific, could have stimulated positive anomalies over NCP and weakened the East Asia trough. Thus, it can be observed that, among many external reasons for the extreme haze in 2014, only the pre-autumn Pacific SSTA was distributed similarly in 2013. The EA/WR Rossby wave train was the prominent circulation contributing to  $WHD_{NCP}$  in 2013, with a source located over the central-north Atlantic. We speculate that the air-sea interaction over north Atlantic excited the EA/WR pattern in the atmosphere and influenced  $WHD_{NCP}$  remotely. The correlation coefficients between the EA/WR index and the pre-autumn SST in Atlantic were calculated and were significantly positive to the south of Greenland (Figure S9b). When the SSTA to the south of Greenland was positive, the responses similar to EA/WR occurred in the atmosphere. The pre-autumn SSTA in the Atlantic in 2013 was similar to that shown in Figure S9b and might have remotely impacted  $WHD_{NCP}$  via the EA/WR pattern. It should be noted that the SSTA of the key region in the Atlantic was negative and had an adverse effect on  $WHD_{NCP}$  in 2014.

From the point of facilitating a larger amount of  $WHD_{NCP}$ , the associated circulations and external forcings in 2013 were different from that in 2014, but the serious situations of haze were almost the same. **In our study, we assumed that the energy consumption linearly increased in the recent years. On such hypothesis, the human activities mainly impacted the long-term trend of  $WHD_{NCP}$ . After removal of the linear trend, the interannual variability of haze pollution should**



**be mainly the result of climatic anomalies.** The Shangdianzi site is the only GAWS in North China and was chosen to reflect the natural or background situation of the atmosphere. The mean mass concentrations of PM<sub>2.5</sub> in winter from 2004 to 2014 are plotted in Figure 11. **The concentration in winter 2013 increased abruptly up to nearly twice that in 2010 and 2014 and was the highest in the observation history that broke down our assumption.** Furthermore, the PM<sub>2.5</sub> concentration of an urban site, Blaolian station, was also much higher than 2010 and 2014. **Even the anomalous circulations were not benefit enough for haze occurrence, the joint effect of highest pollution emissions and climate conditions could result in the serious haze event.** Documented by these three case studies, the influences of the highest concentrations of PM<sub>2.5</sub> were the fundamental cause, and the associated with atmospheric anomalies and external forcings played key roles in the severe haze pollution. In this study, we focused on the roles of climate conditions and did not discuss the impact of human activities deeply that should be researched in the future work. To separate the contributions quantitatively by numerical models or advanced statistical approaches would be a meaningful task that was helpful to the interpretation of mechanism and the seasonal prediction (Yin et al. 2016b). In the case studies, 2010 and 2014 exhibited approximately equal PM<sub>2.5</sub> concentrations of the background atmosphere, but the associated circulations and external forcings in 2010 were still slightly different from those in 2014. It is possible that not all of the above factors might be found in a specific case study, i.e., a few of these effective factors played the essential roles and led to lead to the characteristics of that case. A brief summary of the impacts of these factors on WHD<sub>NCP</sub> is offered in Table 2.....

**5. In Line 10: inappropriate adjective “highest”.**

**Reply:**

The error has been corrected.

**Revision:**

.....The winter (December–February) haze days over the North China Plain (WHD<sub>NCP</sub>) in 2014 were the most in the past 30 years.....



# Understanding Severe Winter Haze ~~Events~~ ~~Pollution~~ in the ~~North-Central~~ North China Plain in 2014: Roles of Climate Condition Anomalies

Zhicong Yin<sup>12</sup>, Huijun Wang<sup>123</sup>, Huopo Chen<sup>231</sup>

<sup>1</sup> Key Laboratory of Meteorological Disaster, Ministry of Education / Joint International Research Laboratory of Climate and Environment Change (ILCEC) / Collaborative Innovation Center on Forecast and Evaluation of Meteorological Disasters (CIC-FEMD) Key Laboratory of Meteorological Disaster, Nanjing University of Information Science & Technology, Nanjing 210044, China

<sup>2</sup> Nansen-Zhu International Research Centre, Institute of Atmospheric Physics, Chinese Academy of Sciences, Beijing, China

<sup>3</sup> Climate Change Research Center, Chinese Academy of Sciences, Beijing, China

Correspondence to: Zhicong Yin (yinzhc@163.com)

**Abstract.** Atmospheric pollution has become a serious environmental and social problem in China. The winter (December–February) haze days over the ~~North-Central~~ North China Plain (WHD<sub>NCP</sub>) in 2014 ~~was~~ ~~were~~ the highest most in the past 30 years. In addition to anthropogenic influence, the roles of climate anomalies were also vital. Thus, it is necessary to analyze the anomalous atmosphere circulations associated with haze atmospheric pollution of this year in detail. Near surface, the weaker East Asian winter monsoon pattern, inducing southerly over North China Plain, could aggravate the situation of haze. On the lower and middle troposphere, Taking the anti-cyclone circulation over North China as an intermediary, the positive phases of the East Atlantic/West Russia (EA/WR), the Western Pacific (WP) and the Eurasia (EU) patterns led to a worse diffusivity of local stable atmosphere that contributed to a larger number of WHD<sub>NCP</sub>. In 2014, these three patterns could be recognized from the wind anomalies in the lower troposphere, ~~which can influence WHD<sub>NCP</sub>.~~ The pre-autumn (September–November) Arctic sea ice (ASI) anomalies over the Eastern Hemisphere and the warmer winter surface over Eurasia might have induced or intensified the positive EA/WR pattern in 2014. These two external forcings, together with the pre-autumn sea surface temperature anomalies in the Pacific, might have also stimulated or enhanced the positive EU-like patterns. The anomalous surface temperature in autumn 2014 was efficient in intensifying anomalous circulations such as the positive phase of the WP pattern. The opposite case of minimum WHD<sub>NCP</sub> in 2010 further supports the

mechanism of how EA/~~WA-WR~~ and WP patterns and associated external factors [altered the local climate conditions to](#) impact the WHD<sub>NCP</sub>.

## 1. Introduction

Related to booming economic development, atmospheric pollution has become a serious environmental and social problem in China (Ding et al. 2014; Wang et al. 2016). Particularly after the persistent heavy fog and haze events in January 2013, haze pollution has become more severe (Zhang et al. 2014; Zhao et al. 2014; Li et al. 2015) and has presented certain negative effects on human health (Yin et al. 2011; Chen et al. 2013). The ~~North Central~~North China Plain (NCP), a location in which the population density is quite high, was one of three haze-prone regions in China. The [winter \(December–February\)](#) haze pollution over NCP (34–43°N, 114–120°E) in 2013 and 2014 was the most serious of these events in the past 30 years (Yin et al. 2015a). Therefore, the objective of this study was to examine the related [climate conditions \(i.e., atmospheric circulation anomalies and external forcings\)](#) that were responsible for the extreme haze ~~events pollution that occurred in winter (December–February)~~ 2014.

[There is no doubt that the anthropogenic emissions were the fundamental cause for the long-term variation of haze days in eastern China \(Wang et al. 2013\). The enormous energy consumption supplied enough particulates, so the atmosphere tended to reach saturation. Thus, the impact of meteorological conditions is highlighted and the climate conditions are also vital contributors to the interannual variation of haze \(Liao et al. 2014\). For example, the joint effect of fast increase of total energy consumption, rapid decline of Arctic sea ice extent and reduced precipitation and surface winds intensified the haze pollution in central North China after 2000 \(Wang et al. 2016\). In addition to pollutant emission, meteorological conditions are also vital contributors to haze occurrence \(Liao et al. 2014; Wang et al. 2016\).](#)—Early studies documented that the East Asian winter monsoon (EAWM) had weakened after 1986, which led to an increase of winter haze days (WHD) over NCP (WHD<sub>NCP</sub>) (Yin et al. 2015a; Yin et al. 2015b; Li et al. 2015). The decline of the preceding autumn (September–November) Arctic Sea Ice (ASI) from 1979 to 2012 greatly intensified haze pollution in eastern China, the variance contribution of which was 45–67% (Wang et al. 2015a). ~~Another external forcing, s~~Sea surface temperature (SST) over the subtropical

western Pacific (SWP); showed significantly negative correlation with  $WHD_{NCP}$ . SWP-SST weakened EAWM circulation, leading to a favorable environment for haze with ~~high static stability~~ stable atmosphere and potential for hygroscopic growth (Yin et al. ~~2015~~2016a).

The ~~obvious~~ local anti-cyclone anomaly around NCP was the most prominent circulation related to  $WHD_{NCP}$  (Yin et al. ~~2015~~2016a; Chen et al. 2015) and was located near the bonding area of two continental Rossby waves, i.e., Eurasia (EU) and East Atlantic/West Russia (EA/WR) patterns. The EU pattern, as defined by Wallace et al. (1981), originated from the high-latitude polar region. The EU positive phase showed negative centers over the polar region (70–80°N, 60–90°E) and the Japan Sea (35–45°N, 120–140°E), and a positive center over Mongolia and North China (45–55°N, 90–110°E), which accounted for the severe drought in 2014 (Wang et al. 2015b). Another Eurasian teleconnection, known as the EA/WR pattern (Barnston et al. 1987), was composed of negative centers over Central-North Atlantic and to the north of the Caspian Sea, and positive centers over Europe and North China. The positive phase of these two continental Rossby wave trains might have led to significant warming over the northern portion of Eastern Asia (Liu et al. 2014), indicating weaker cold air. Therefore, we speculated that external forcings such as the SST, ASI and land surface temperature (TS) might impact  ~~$WHD_{NCP}$  remotely by inducing~~ teleconnection patterns in the atmosphere and then the teleconnection patterns could alter the local climate anomalies to modulate the  $WHD_{NCP}$  remotely. Climate research on haze pollution in China is quite a new endeavor but is still insufficient, especially with respect to investigation into the mechanism that causes extreme haze events. Thus, the ~~roles impact~~ of climate ~~change anomalies~~ on the ~~persistent~~ winter haze in 2014 over NCP ~~were~~ investigated in this study and ~~were~~ expected to improve prediction skill for  $WHD_{NCP}$ .

The remainder of this paper is organized as follows. The data and methods are clearly explained in Section 2. The climatic reality of severe  $WHD_{NCP}$  in 2014 and associated atmospheric circulations are analyzed in Section 3. Section 4 describes investigation of the physical mechanism using the singular value decomposition (SVD) technique. Brief conclusions and selected discussions are presented in Section 5.

## 2. Datasets and methods

The China ground observations from 39 NCP stations (Figure 1) collected by the National Meteorological Information Center of China from 1979 to 2015 were used to reconstruct the climatic WHD data, referred to Yin et al. (2016). Due to the After-quality and temporal range of the data-control, only four rural stations were qualified and selected (white circles in Figure 1), ~~and the datasets tended to represent the characteristics of urban haze~~. The weather measurements included relative humidity, visibility and wind speed that were collected four times per day, i.e., 02:00 local time (LT), 08:00 LT (00:00 UTC), 14:00 LT, and 20:00 LT. In this work, haze is recognized when visibility falls below a certain threshold and the relative humidity is less than 90%. After excluding other weather phenomena that affect visibility, a day with haze occurring at any time is defined as a haze day. Most of the visibility observations have switched from manual to automatic since Jan 1<sup>st</sup>, 2014, but the trial stations coded 54511, 54527 and 54623 were switched in 2013. Thus, the visibility threshold is 10 km before Jan 1<sup>st</sup>, 2014 for most stations, but before Dec 1<sup>st</sup>, 2013 for the trial stations. After the switch, the threshold is 7.5 km, according to the China Meteorology Administration's notification (2014). To a certain extent, the WHD data of 2013 and 2014 are more qualitative than quantitative. To avoid continuity problems, the haze data for these two years were processed using composite analysis instead of correlation analysis in this study.

Haze is a multidisciplinary phenomenon that can be represented by visibility and humidity in meteorology, and by the concentration of the atmospheric composition in environmental science. In recent years, the atmospheric compositions involving the concentrations of SO<sub>2</sub>, NO, NO<sub>2</sub>, NO<sub>x</sub>, CO, O<sub>3</sub>, PM<sub>2.5</sub> (by TEOM 1400a) and nephelometric turbidity (NEP) were measured in Shangdianzi and Baolian, (an urban site in Beijing, Zhao et al. 2011) (~~Zhao et al. 2011~~). The detailed atmospheric composition datasets were collected four times per day from Dec 1<sup>st</sup>, 2014 to Feb 28<sup>th</sup>, 2015. The hourly PM<sub>2.5</sub> data from 2004 to 2015 were observed at Shangdianzi Station, one of the six regional global atmospheric watch stations (GAWS) in China and from 2008 to 2015 at Baolian Station. Shangdianzi Station is located at 40°39'N, 117°7'E and at a height of 293.3 m, which shelters it from human activities and pollution sources. As the only GAWS in North China, the atmospheric composition at this location was chosen to best reflect the natural state or rather the background conditions of the atmosphere (Yao et al. 2012). The PM<sub>2.5</sub> data were monitored every 5 minutes using two methods: tapered element

95 oscillating microbalance (TEOM) and  $\beta$ -ray (since 2013).

In China, the temporal range and quality of the observed atmospheric compositions cannot support climatic haze research. To demonstrate the representation of haze data reconstructed primarily by visibility, the hourly visibility and concentration of the atmospheric composition were shown, and the correlation coefficients were computed (Figure 2S1). In addition to significantly positive correlation with  $O_3$ , the correlation coefficients between visibility and seven compositions were all negative and exceeded the 99.99% confidence level in winter 2014.  $PM_{2.5}$  was the main reason for haze pollution, and the correlation coefficients with visibility in Beijing were  $-0.51$  (Baolian) and  $-0.48$  (Shangdianzi). When visibility was less than 7.5 km and 1 km, the mean  $PM_{2.5}$  mass concentrations at Baolian were approximately greater than 100 and  $200\mu\text{g}/\text{m}^3$ , respectively. Thus, the tendency and magnitude both showed that the derived haze datasets not only agreed with the meteorological standard but also satisfactorily represented the concentration of the atmospheric composition.

105 Monthly atmospheric data such as wind, geopotential height, temperature and sea level pressure (SLP) are derived from the National Centers for Environmental Prediction/National Center for Atmospheric Research (~~NCEP/NCAR~~) global reanalysis dataset with a horizontal resolution of  $2.5^\circ \times 2.5^\circ$  collected from 1979 to 2015 (Kalnay et al. 1996). [The monthly mean planetary boundary layer height \(PBLH,  \$1^\circ \times 1^\circ\$ \) was derived from the ERA-Interim dataset \(Dee et al. 2011\)](#). The monthly mean Extended Reconstructed SST (ERSST) datasets with a horizontal resolution of  $2^\circ \times 2^\circ$  collected from 1979 to 2015 were obtained from the National Oceanic and Atmospheric Administration (NOAA) (Smith et al. 2008). The ASI extent was calculated using the ASI concentration data from Hadley Center's HadISST1 with a resolution of  $1^\circ \times 1^\circ$  collected from 1979 to 2015 (Rayner et al. 2003). The EA/WR and WP indices were computed by the NOAA climate prediction center according to the Rotated Principal Component Analysis (~~RPCA~~) used by Barnston et al. (1987). The calculation procedure for the EU index was consistent with that of Wang et al. (2015b).

$$\text{EU index} = \left[ -1 \times \overline{H500}_{(70-80^\circ\text{N}, 60-90^\circ\text{E})} + 2 \times \overline{H500}_{(45-55^\circ\text{N}, 90-110^\circ\text{E})} - 1 \times \overline{H500}_{(35-45^\circ\text{N}, 120-140^\circ\text{E})} \right] / 4$$

115 where H500 represents the geopotential height at 500 hPa and overbars denote the area average.

To verify the covariability between the air and external forcings, i.e., SST, ASI and TS, SVD and correlation analyses were applied after linear trends were removed. [To some extent, the energy consumption varied continuously and linearly in eastern](#)

China and the socio-economic components of WHD<sub>NCP</sub> could be removed primitively by detrending, and then the interannual variability of haze pollution should be mainly the result of climatic anomalies. The anomalies in 2010, 2013 and

120 2014 were calculated relative to the climatic mean of 1979-2012. The site WHD data were converted into grids using the Cressman interpolation (Cressman, 1959), and WHD<sub>NCP</sub> was computed as the mean value of the grid data.

### 3. Variations of WHD<sub>NCP</sub> and associated atmospheric circulations

According to Figure 32, WHD<sub>NCP</sub> from 1979 to 2012 can be divided into two decadal stages, i.e., the first stage from 1979 to 1992 with an average of 45.1 days and the second decade from 1993 to 2012 with an average of 34.5 days. It is obvious that

125 WHD<sub>NCP</sub> exhibited rapid increase since winter 2010 with a large trend of 7.36 d/yr. NCP is a haze-prone area in which WHD is distributed nonuniformly (Figure 4a3a). Two regions exhibited greater WHD: the plain to the east of Taihang Mountains and to the south of Yan Mountains (PETSU) and the south of Shandong Province. As shown in Figure 1, there were four rural stations, three of which were located near the Yan Mountains and were corresponding to less WHD. Another rural site was near the boundaries of Shandong and Henan (BSH) and also resulted in less WHD. Figure 34b shows the WHD

130 anomalies in 2014 with respect to 1979–2012. In addition to a few sites, a larger number of WHD occurred, especially on the border of Shandong and Henan BSH (rural area) and the northeast of Hebei. It is interesting to note that WHDs in these two regions show significant increases, filling up the climatic WHD valley as shown in Figure 4a3a. As a result, the haze-prone stations area joined together, indicating that the haze pollution was more serious in this region. Actually, the fast increase of WHD in rural area was an obvious reflection of the severe haze disaster in recent years. At the same time, a

135 larger number of WHD occurred on PETSU and the south of Shandong Province. Recently, the haze pollution has become increasingly serious, as shown by the number of haze days and its coverage. The percentages of sites with greater than 30 and 60 hazy days were 71.8% and 51.3%, respectively, in 2014. As shown in Figure S12, the mean PM<sub>2.5</sub> mass concentrations in Beijing were approximately above 100µg/m<sup>3</sup> on hazy days, which indicated s serious pollution in 2014.

140 Although data continuity was influenced by the switch of the observation method in 2013, the observation that WHD<sub>NCP</sub> in 2014 was greater than before showed robustness. Thus, it is reasonable to treat the year 2014 as a typical case for haze



pollution over this region. As shown in Figure 32, NCP experienced the least WHD in 2010, which could be analyzed as an inverse case of the extreme haze phenomena.

~~In winter, the negative SLP anomaly in the Siberia region and the Chinese Mainland and the positive SLP anomaly over the West Pacific led to a reduced pressure gradient and weakened EAWM (Figure 5a). The weaker EAWM induced the southeasterly anomaly and reduced the surface wind speed (Figure 5c), indicating weaker cold air and a warmer land surface over NCP (Figure 5a). Influenced by the circulations with weaker cold air, horizontal diffusion of the atmospheric particulates was impeded, which was beneficial for haze occurrence. In the winter of 2014, the surface temperature of the Asian continent was higher, illustrating that the EAWM was weaker from the source region to its south margin (Wang et al. 2015). The continental and oceanic SLP anomalies stimulated a significant southerly anomaly to the north of 50°N, blocking the cold air from high latitudes (Figure 5b). A southerly and smaller surface wind speed anomaly also occurred over the coastal area in the east of China (Figure 5d), resulting in more WHD<sub>NCP</sub>.~~

In the lower and middle-high layers of the troposphere, the correlation fields between WHD<sub>NCP</sub> and H500 (UV850) represented obvious EA/WR and WP patterns (Figure 46a–b). The EA/WR pattern originated from the north-central Atlantic and propagated through Europe, the north of Caspian Sea and North China (Barnston et al. 1987; Liu et al. 2014). The WP pattern showed two activity centers, i.e., the broad area of Southeast Asia and the northwest Pacific and the Kamchatka Peninsula (Barnston et al. 1987). In addition to EA/WR, the EU pattern was another continental Rossby wave train over Eurasia, which significantly impacted the climate of East Asia (Liu et al. 2014). Although the EU pattern was unclear in Figure 64a–b, it can be recognized distinctively from the anomalous circulations in 2014 (Figure 64c). The correlation coefficients between WHD<sub>NCP</sub> and these three pattern indices were calculated (Table 1). After detrending, WHD<sub>NCP</sub> showed significant positive correlation with both the EA/WR and WP patterns, indicating the remote impact on WHD<sub>NCP</sub> from land and sea. The correlation between EU and WHD<sub>NCP</sub> was initially significantly positive but became insignificant after detrending. Considering that EU could be recognized from low, middle and high layers in winter 2014, the EU pattern was still treated as a possible circulation correlated with WHD<sub>NCP</sub>. These teleconnection patterns might contribute to WHD<sub>NCP</sub> by impacting the pivotal and local anti-cyclone anomalies (i.e., the local climate conditions) over NCP (Figure 4a–b). The

165 deep and broad positive anomalies ~~confined the particles within~~ resulted in a thinner boundary layer by suppressing vertical  
movement and progressed easterly to weaken the East Asia Jet Stream (EAJS); indicating weaker meridional cold air. Near  
surface, the negative SLP anomalies in the Siberia region and the Chinese Mainland and the positive SLP anomalies over the  
West Pacific led to a reduced pressure gradient and weakened EAWM (Figure 5a). The weaker EAWM induced the  
southeasterly anomalies and reduced the surface wind speed (Figure 5b), indicating weaker cold air and warmer land surface  
170 over NCP (Figure 5a). Influenced by the circulations with weaker cold air, horizontal diffusion of the atmospheric  
particulates was impeded. Near NCP, the anomalous anti-cyclone also existed that illustrated weaker vertical motion. The  
main physical process was that the climate teleconnection patterns altered the local climate conditions, and then influenced  
the diffusivity of the local atmosphere. That is, when the positive pattern of EA/WR, WP and EU occurred together or partly,  
the anomalous anti-cyclone over NCP and Japan Sea was enhanced from surface to the middle troposphere, thus, the  
175 convection or vertical motion was confined. The southerly anomalies on the left side of this anti-cyclone weakened the cold  
air and wind speed, but brought about humid flow. Under such local climate anomalies, the vertical and horizontal diffusion  
of atmospheric particulates were both restricted and then the pollutant gathered in a narrow space that resulted in the  
occurrence of haze.

In winter 2014, many extreme climatic events occurred, such as severe drought and high temperatures in NCP (Wang et al.  
180 2015). Corresponding external forcings should be observed as the background of these extreme synoptic and climatic events,  
which might persistently impacted the winter atmospheric circulations, and leading to an irregular distribution of  
teleconnection patterns in winter. It should be noted that EA/WR pattern in winter 2014 was distributed slightly westwards  
and broadly. Nevertheless, the three eastern centers of EA/WR, WP and EU patterns could be recognized ~~clearly~~ (Figure 64c).  
The linkage anti-cyclone of these three teleconnection patterns was enhanced and modulated the local climate conditions.  
185 The NCP area was influenced by the anomalous high resulting in lower PBLH (Figure 6). The southerly at the high latitudes  
deadened the cold air from its main source, so the atmospheric matters gathered easily. Near surface, the negative SLP  
anomalies occupied the whole Asian continent and Japan Sea that weakened the continental cold high and stimulated  
significant southerly anomalies to the north of 50°N with the weaker Aleutian low. The weaker EAWM circulations near

190 surface blocked the cold air from high latitudes and resulted in warmer surface (Wang et al. 2015). There were positive SLP  
anomalies over South China Sea and East China Sea that induced southerly and smaller surface wind speed over the coastal  
area in the east of China (Figure 5c—d). The diffusivity of atmosphere over the NCP was limited, so the high pollutant  
emissions were concentrated in a narrow space and severe haze events occurred easily. Large scale  $\bar{C}$  circulations, such as the  
negative phase of EA/WR and WP, were quite clear in 2010 (Figure 6d), ~~leading to a favorable environment for diffusion~~  
~~with stronger cold air and vertical movement.~~ Near surface, the anomalous circulations were distributed similarly but almost  
195 opposite, i.e., the stronger continental cold high and oceanic low (Figure 5e), the northerly and stronger surface wind over  
NCP (Figure 5f), and the higher PBLH (Figure 6). The atmospheric diffusivity was heightened by the stronger cold air and  
vertical movement. This observation further supports the speculation that the anomalous EA/WR and WP patterns  
contributed to significant changes in  $WHD_{NCP}$  by altering the local climate conditions. The anomalies of the EU pattern in  
winter 2010 were not as significant as those in 2014. As shown by Table 1, the relationship between  $WHD_{NCP}$  and the EU  
200 index weakened after detrending, illustrating that the correlation was much weaker than the other two patterns.

#### 4. Possible mechanisms for the winter haze in 2014

In the above discussion, we addressed the associated circulations that were characterized by EA/WR, WP and EU patterns  
and that contributed to the extreme haze pollution in 2014. Wang et al. (2015a) found that the pre-autumn ASI could  
significantly impact the WHD in the east of China. As another efficient external forcing, the negative SWP-SST anomalies  
205 (SSTA) markedly intensified  $WHD_{NCP}$  (Yin et al. 2016a5e). Thus, the question arises as to whether these factors could have  
caused the extreme haze pollution that was measured in 2014.

Since 1979, the pre-autumn ASI declined substantially, which might impact the winter climate of East Asia (Liu et al. 2012).  
Furthermore, this decreasing trend of the ASI intensified from 2006 (Wang et al. 2015a), ~~attracting global attention.~~ The  
relationship between the pre-autumn ASI and the circulations was analyzed using the SVD method, explaining 51.6% and  
210 17.9% of the variance by the first (SVD1) and second (SVD2) mode, respectively. The correlation coefficient of the first  
temporal series was 0.76, which was significantly above the 99% confidence level. The excited anti-cyclonic (A) or cyclonic

(C) activity centers of H500 in winter were located over the north Atlantic, Europe, to the north of Caspian Sea and around Mongolia and North China, which appeared as the positive phase of the EA/WR pattern (Figure 77a). The corresponding pre-autumn ASI, with more sea ice (SI) over the Barents Sea, Kara Sea and Laptev Sea (BKLSI) and less SI in the East Siberian Sea (ESSI) could have contributed to the positive EA/WR pattern (Figure 77b). The anomalous ASI of the Eastern Hemisphere in 2014 was similar to that shown in Figure 77b. According to the SVD results, the pre-autumn ASI anomalies in 2014 might have triggered the EA/WR pattern in the atmosphere, especially the anomalous high over NCP, and led to greater WHD<sub>NCP</sub>. In autumn 2010, less BKLSI and more ESSI (Figure S42) occurred, which might have induced less WHD over NCP.

In winter 2014, the TS anomalies of the broad region of Eurasia (40–70°N) were obviously positive. EA/WR is a famous continental teleconnection, and a significant land-air interaction could influence the EA/WR pattern. To illustrate this concept, an SVD analysis was performed between the detrended and normalized winter TS and H500 (Figure 88). The explained variance (EV) and correlation coefficient of the first component were 53.3% and 0.73, respectively. The spatial coefficients of TS were distributed similarly with TS anomalies in 2014. The associated circulations displayed three anomalous centers, i.e., a positive center over Europe, negative anomalies to the north of Caspian Sea, and another positive center over Mongolia and North China, which were also the three atmospherically active centers of EA/WR on the continent that occurred in winter 2014 (Figure 5c). These results indicated that the TS anomalies of winter 2014 could have induced or intensified the positive EA/WR phase and resulted in the extreme WHD<sub>NCP</sub> case in 2014. In winter 2010, the cooler land surface of mid-latitude Eurasia (Figure S23) could have contributed to the negative EA/WR phase. The diagnostic analyses of two inversely extreme WHD<sub>NCP</sub> cases enhanced the relationship between the winter mid-latitude Eurasia TS and WHD<sub>NCP</sub>.

Figures 77 and 88 also show negative anomalies over the polar area (70–80°N, 60–90°E) and a positive center over Mongolia and North China (45–55°N, 90–110°E), which can be recognized as the positive EU phase. When BKLSI was above normal and ESSI was below normal or the surface of mid-latitude Eurasia was warmer, these two centers could be stimulated or enhanced, and represented favorable circulations for haze occurrence. Prior to this study, Yin et al. (20165e) found that the pre-autumn SSTA of the Pacific excited atmospheric responses, including the anti-cyclone anomalies over North China, and

resulted in more  $WHD_{NCP}$ . The SST in October and November (ON) and winter H500 were decomposed using the SVD technique to reveal the main relationships. The [explained variance](#)EV and the correlation coefficient of the first component were 60.2% and 0.73, respectively. An EU-like pattern occurred in the first mode of H500, i.e., cyclonic anomalies over the polar area and anti-cyclonic anomalies over Mongolia and North China (Figure [99a](#)). The associated SST was cooler over the northwest Pacific, involving Kuroshio and its extension, and warmer over the central-east Pacific and Alaska Gulf (Figure [99b](#)). Another atmospheric response was the weaker East Asia trough, indicating weaker EAWM and cold air. Figure [9e-9c](#) shows the ON SSTA of the Pacific in 2014, which appeared to be similar to the SST SVD1 distribution and stimulated haze-prone responses. In 2010, the ON SSTA in the Pacific did not show a well-organized opposite pattern (Figure [S43](#)), but a cooler SST was observed on the central-east Pacific and Alaska Gulf, which were of benefit to haze occurrence.

Both EA/WR and EU were continental teleconnection patterns that propagated over Eurasia. In contrast, the WP pattern was located over the junction of the marine and mainland areas, and its positive phases were composed of a broad positive center over the northwest Pacific and Southeast Asia and a negative center over Kamchatka Peninsula (Barnston et al. 1987). From Table 1, the stronger WP positive phase could have contributed to more  $WHD_{NCP}$  and could also have been partially responsible for the severe haze event in 2014. To identify the causes of such circulations, we performed an SVD analysis between winter H500 and pre-autumn TS, with [explained variance](#)EV values of 39.8% and 20.7%, respectively, for SVD1 and SVD2. The results of SVD2 showed significant anomalies in the two centers of the positive WP pattern and anomalous TS distributed from the southwest to the northeast in Eurasia (Figure [4910](#)). The correlation coefficient of the SVD2 time series was 0.62, exceeding the 99% confidence level. Similar to the SVD2 representation, two “southwest to northeast” anomalous TS distributions also occurred in autumn 2014, i.e., negative anomalies from the Caspian Sea to Baikal Lake and a positive anomalous belt from Southwest China to Northeast China (Figure [4910c](#)). Referring to SVD2, these “southwest to northeast” TS anomalies could have induced atmospheric responses over the junction of the Pacific and Asian land, which resembled the WP pattern and impacted the local circulations over the NCP area. In autumn 2010, the positive belt of TS from the Caspian Sea to Baikal Lake was significant, and the land surface of the Tibet Plateau was warmer than normal (Figure [S54](#)). These two anomalies were dramatically inverted with the SVD2 results and could have stimulated a negative

260 WP pattern. As argued by two opposed cases, the mechanism for how the EA/~~WA-WR~~ and WP patterns and associated external factors impacted the  $WHD_{NCP}$  were confirmed.

## 5. Conclusions and discussions

265 Except for a few sites, haze pollution over NCP in winter 2014 was the severest in the past 30 years. On the ~~BSH border of Shandong and Henan area~~ and the northeast of Hebei, WHD increased significantly and ~~filled up the climatic WHD valley invaded into the rural area~~, illustrating a joint and broad severe haze-prone region. ~~The  $PM_{2.5}$  concentration at a GAWS and an urban site were almost equal in winter 2010 and 2014, so there was no evidence that the emissions were more in 2014 than 2010. The climate anomalies played key roles in the formation of heavy haze pollution case in 2014. On the lower and middle troposphere, Taking the anti-cyclone anomalies over North China as an intermediary,~~ the positive phases of EA/WR, WP and EU patterns ~~modulated the local anti-cyclone anomalies over North China led to a stable atmosphere, which was beneficial for haze occurrence.~~ The anti-cyclone anomalies over East Asia not only resulted in stable atmospheric stratification and a thinner boundary layer but also led to a southeasterly anomaly that weakened the cold air but enhanced the moisture transport. ~~The atmospheric matters would accumulate easily both on the vertical and horizontal direction.~~ In winter 2014, ~~the~~ teleconnection patterns, such as EA/WR, EU and WP, combined to ~~alter the local climate conditions to~~ contribute to the extreme haze case. SVD analyses indicated that the pre-autumn ASI anomalies of the Eastern Hemisphere and the warmer winter surface of Eurasia could have induced or intensified the responses in the atmosphere, resembling a positive EA/WR pattern. These two external forcings, together with the SSTA in Pacific (i.e., cooler in the northwest Pacific and warmer in the central-east Pacific and Alaska Gulf) might stimulate or enhance positive EU-like patterns. In autumn 2014, the “southwest to northeast” anomalous TS belts were other factors that efficiently intensified the haze pollutions, which resulted in a positive phase of the WP pattern. The case of 2010, with the least  $WHD_{NCP}$ , was diagnosed as an opposite case, which further supports the speculation that the anomalous EA/WR and WR patterns and associated external forcings have a significant impact on  $WHD_{NCP}$ . ~~Additionally, as pointed out by Wang et al. (2015), the Asian high temperature and drought from summer in 2014 was an extreme climate event. Our studies proved that this previous extreme climate event~~

270

275

280

possibly contributed to the serious haze event in the following winter.

The rapid increase of  $WHD_{NCP}$  began in January 2013, and in winter 2013 and 2014,  $WHD_{NCP}$  was significantly greater than before. The  $WHD_{NCP}$  in 2013 and 2014 was greater than 50 days and almost equal to each other (Figure 22). Therefore, the causes of serious haze in 2013 should also be discussed. ~~The anomalous circulations in winter 2013 were not as favorable for haze conditions as those in 2014.~~ The EA/WR pattern was well organized and showed a positive phase that was distributed slightly eastwards (Figure S56). Influenced by the upper EA/WR pattern, the surface wind speed was slower and the PBLH was lower, illustrating the horizontal and vertical diffusivity of the atmosphere was weaker (Figure S7). The EU and WP patterns were unclear. The source region of EU even showed characteristics of a negative phase. ~~From the perspective of anomalous circulation, the main cause contributing to serious  $WHD_{NCP}$  in 2013 was the remote impact of the EA/WR Rossby wave and appeared weaker than that in 2014.~~ According to the 2010 and 2014 case studies, the proceeding and simultaneous external forcings could have impacted the  $WHD_{NCP}$ . In contrast, the pre-autumn ASI and TS and winter TS in 2013 did not show features similar to those in 2014 (Figure S68). The pre-autumn Pacific SSTA, which was slightly negative in the northwest Pacific and positive in the Alaska Gulf and central-east Pacific, could have stimulated positive anomalies over NCP and weakened the East Asia trough. Thus, it can be observed that, among many external reasons for the extreme haze in 2014, only the pre-autumn Pacific SSTA was distributed similarly in 2013. The EA/WR Rossby wave train was the prominent circulation contributing to  $WHD_{NCP}$  in 2013, with a source located over the central-north Atlantic. We speculate that the air-sea interaction over north Atlantic excited the EA/WR pattern in the atmosphere and influenced  $WHD_{NCP}$  remotely. The correlation coefficients between the EA/WR index and the pre-autumn SST in Atlantic were calculated and were significantly positive to the south of Greenland (Figure S97b). When the SSTA to the south of Greenland was positive, the responses similar to EA/WR that occurred in the atmosphere. The pre-autumn SSTA in the Atlantic in 2013 was similar to that shown in Figure S79b and might have remotely impacted  $WHD_{NCP}$  via the EA/WR pattern. It should be noted that the SSTA of the key region in the Atlantic was negative and had an adverse effect on  $WHD_{NCP}$  in 2014.

From the point of facilitating a larger amount of  $WHD_{NCP}$ , the associated circulations and external forcings in 2013 were different from that in 2014 ~~and slightly weaker synthetically to a certain extent,~~ but the serious situations of haze were almost

~~the same. The climate conditions influenced haze weather on the premise that pollutant emissions were high. In our study, we assumed that the energy consumption linearly increased in the recent years. On such hypothesis, the human activities mainly impacted the long-term trend of WHD<sub>NCP</sub>. After removal of the linear trend, the interannual variability of haze pollution should be mainly the result of climatic anomalies.~~ The Shangdianzi site is the only GAWS in North China and was chosen to reflect the natural or background situation of the atmosphere. The mean mass concentrations of PM<sub>2.5</sub> in winter from 2004 to 2014 are plotted in Figure 114. The concentration in winter 2013 ~~increased abruptly up to nearly twice that in 2010 and 2014 and~~ was the highest ~~in the observation history that broke down our assumption.~~ Furthermore, the PM<sub>2.5</sub> concentration of an urban site, Blaolian station, was also much higher than 2010 and 2014. Even the anomalous circulations were not benefit enough for haze occurrence, the joint effect of highest pollution emissions and climate conditions could result in the serious haze event. ~~and nearly twice that in 2010 and 2014. The reasons for the serious haze pollution in 2013 were more compositive and complicated. Documented by these three case studies,~~ ~~the influences of the highest concentrations of PM<sub>2.5</sub> were the fundamental cause, and the~~ associated with atmospheric anomalies and external forcings ~~added up and contributed to~~ played key roles in the severe haze pollution. ~~Compared with 2013, the concentrations measured by the two methods both decreased dramatically in 2014, indicating that the climate conditions accounted for a greater proportion.~~ In this study, we focused on the roles of climate conditions and did not discuss the impact of human activities deeply that should be researched in the future work. To separate the contributions quantitatively by numerical models or advanced statistical approaches would be a meaningful task that was helpful to the interpretation of mechanism and the seasonal prediction (Yin et al. 2016b).

~~Although the reconstructed haze datasets showed good representativeness for the meteorological phenomena and environmental disasters, the data in 2013 and 2014 were more qualitative than quantitative. To avoid a continuity problem, the haze data of these two years were processed using composite analysis instead of correlation analysis in this study.~~ In the ~~three~~ case studies, 2010 and 2014 exhibited approximately equal PM<sub>2.5</sub> concentrations of the background atmosphere, ~~which was close to the mean value, but the concentration in 2013 was almost twice as large.~~ Compared with 2013, the climate conditions accounted for a greater proportion among the reasons for haze in 2010 and 2014. Even so, ~~but~~ the associated



335 circulations and external forcings in 2010 were still slightly different from those in 2014. It is possible that not all of the above factors might be found in a specific case study, i.e., ~~only~~ a few of these factors played the essential roles and led effectively led to the characteristics of that case. ~~The climate change influence on haze weather was based on the premise that the pollutant emission was high and slowly changing in recent years, whose influence was removed simply by detrending. For peculiar cases with dramatically changing atmospheric particles, such as 2013, the variation of pollution emission should be investigated.~~ A brief summary of the impacts of these factors on WHD<sub>NCP</sub> is offered in Table 2.

### Acknowledgements

340 This research was supported by the National Natural Science Foundation of China (Grants: 41421004 and 41210007) and CAS-PKU Partnership Program.

### References

Barnston A G, Livezey R E. 1987. Classification, seasonality and persistence of low frequency atmospheric circulation patterns. *Mon. Wea. Rev.*, 115: 1083–1126.

345 Chen H P, Wang H J. 2015. Haze days in North China and the associated atmospheric circulations based on daily visibility data from 1960 to 2012. *J. Geophys. Res. Atmos.* 120(12): 5895–5909 DOI: 10.1002/2015JD023225.

Chen Y, Ebenstein A, Greenstone M, Li H. 2013. Evidence on the impact of sustained exposure to air pollution on life expectancy from China's Huai River policy. *Atmospheric Chemistry and Physics*. 110: 12936–12941

350 China Meteorology Administration. 2014. The notification on the adjustment of haze phenomenon observing provisions and revision of fog-haze observation data in 2013 by Observing and Forecasting Department Division. China Meteorology Administration.

Cressman G. 1959. An operational objective analysis system, *Mon. Wea. Rev.* 87(10): 367–374.

[Dee D P, Uppala S M, Simmons A J, Berrisford P, Poli P, Kobayashi S, Andrae U, Balmaseda M A, Balsamo G, Bauer P, Bechtold P, Beljaars A C M. 2011, The ERA-Interim reanalysis: configuration and performance of the data assimilation system. Q.J.R. Meteorol. Soc., 137: 553—597, DOI: 10.1002/qj.828](#)

355 Ding Y H, Liu Y J. 2014. Analysis of long-term variations of fog and haze in China in recent 50 years and their relations with atmospheric humidity. *Sci. China Ser. D: Earth Sci.* 57: 36–46 (in Chinese)..

Kalnay E, Kanamitsu M, Kistler R, Collins W, Deaven D, Gandin L, Iredell M, Saha S, White G, Woollen J, Zhu Y, Leetmaa A, Reynolds R, Chelliah M, Ebisuzaki W, Higgins W, Janowiak J, Mo KC, Ropelewski C, Wang J, Jenne R, Joseph D. 1996. The NCEP/NCAR 40-year reanalysis project. *Bull. Am. Meteorol. Soc.*, 77: 437–471, doi: 10.1175/1520-0477(1996)077<0437: TNYRP>2.0.CO; 2.

360

Li Q, Zhang R H, Wang Y. 2015. Interannual variation of the winter-time fog–haze days across central and eastern China and its relation with East Asian winter monsoon. *Int. J. Climatol.* 36 (1): 346–354, doi: 10.1002/joc.4350.

Liao X N, Zhang X, Wang Y, Liu W, Du J, Zhao L. 2014. Comparative analysis on meteorological condition for persistent haze cases in summer and winter in Beijing. *Environ. Sci. Technol.* 35(6): 2031–2044 (in Chinese).

365

Liu J P, Judith A. Curry, Wang H J, Mirong Song, Radley M. Horton. 2012. Impact of declining Arctic sea ice on winter snowfall. *Proc. Natl. Acad. Sci.*, 109 (11): 4074–4079. DOI: 10.1073/pnas.1114910109

Liu Y Y, Wang L, Zhou W, Chen W. 2014. Three Eurasian teleconnection pattern: spatial structures, temporal variability, and associated climate anomalies. *Clim Dyn.* 42: 2817–2839

370

Rayner N A, Parker D E, Horton E B, Folland C K, Alexander L V, Rowell D P, Kent E C, Kaplan A. 2003. Global analyses of sea surface temperature, sea ice, and night marine air temperature since the late nineteenth century. *J. Geophys. Res.* 108 (14): 4407 doi: 10.1029/2002JD002670

Smith T, Reynolds R, Peterson T, Lawrimore J. 2008. Improvements to NOAA’s historical merged land–ocean surface temperature analysis (1880–2006). *J. Climat.*, 21: 2283–2296

Wallace J M, Gutzler D S. 1981. Teleconnection in the geopotential height field during the Northern Hemisphere winter. *Mon.*

375

*Wea. Rev.*, 109, 784–812, doi:10.1175/1520-0493(1981)109,0784:TITGHF.2.0.CO;2.

- Wang D Q, Cui T, Si D, Shao X, Li Q Q, Sun C H. 2015. Features and Possible Causes for East Asian Winter Monsoon in 2014/2015. *Meteorological Monthly*. 41(7): 907–914(in Chinese).
- Wang H J, Chen H P, Liu J P. 2015a. Arctic sea ice decline intensified haze pollution in eastern China, *Atmos. Oceanic Sci. Lett.*, 8 (1): 1–9
- 380 Wang H J, He S P. 2015b. The North China/Northeastern Asia Severe Summer Drought in 2014. *Journal of Climate*. 28(17), 6667–668
- Wang H J, Chen H P. 2016. Understanding the recent trend of haze pollution in eastern China: role of climate change, *Atmos. Chem. Phys.*, 16: 4205–4211
- [Wang, Y. S., Yao, L., Liu, Z. R., Ji, D. S., Wang, L. L., Zhang, J. K. 2013. Formation of haze pollution in Beijing-Tianjin-Hebei region and their control strategies. \*Bull. Chinese Acad. Sci.\*, 28, 353–363](#)
- 385 [Wang, Y. S., Yao, L., Liu, Z. R., Ji, D. S., Wang, L. L., Zhang, J. K. 2013. Formation of haze pollution in Beijing-Tianjin-Hebei region and their control strategies. \*Bull. Chinese Acad. Sci.\*, 28, 353–363](#)
- Yao B, Vollmer M K, Zhou L X, Henne S, Reimann S, Li P C, Wenger A, Hill M. 2012. In-situ measurements of atmospheric hydrofluorocarbons (HFCs) and perfluorocarbons (PFCs) at the Shangdianzi regional background station, China, *Atmos. Chem. Phys.*, 12, 10181–10193, doi:10.5194/acp-12-10181-2012, 2012.
- Yin Y, Cheng J, Duan Y, Wei H, Ji R, Yu J, Yu H. 2011. Correlation analysis between the PM<sub>2.5</sub>, PM<sub>10</sub> which were taken in the hazy day and the number of outpatient about breathing sections, breathing sections of pediatrics in Shanghai. *Huan Jing Ke Xue* 32(7): 1894–1898 (in Chinese).
- 390 Yin Z C, Wang H J, GUO W L. 2015a. Climatic change features of fog and haze in winter over North China and Huang-Huai Area. *SCIENCE CHINA Earth Sciences*, 58(8): 1370–1376.
- Yin Z C, Wang H J, Yuan D M. 2015b. Interdecadal increase of haze in winter over North China and the Huang-huai area and the weakening of the East Asia winter monsoon. *Chin. Sci. Bull.* 60(15): 1395–1400 (in Chinese).
- 395 Yin Z C, Wang H J. 2016a. The relationship between the subtropical Western Pacific SST and haze over North-Central North China Plain. *International Journal of Climatology*, 36: 3479–3491, DOI: 10.1002/joc.4570
- [Yin Z C, Wang H J. 2016b. Seasonal Prediction of Winter Haze Days in the North-Central North China Plain, \*Atmos. Chem. Phys.\*, doi:10.5194/acp-2016-691.](#)

400 Zhang R H, Li Q, Zhang R N. 2014. Meteorological conditions for the persistent severe fog and haze event over eastern China in January 2013. *ScienceChina: Earth Sciences*, 57: 26–35. doi: 10.1360/972013-150

Zhao N, Yin Z C, Wu F. 2014. Characteristics of persistent fog and haze process and its forming reason in Beijing. *J. Meteorol. Environ.* 30(5): 15–20 (in Chinese).

Zhao P S, Zhang X L, Xu X F, Zhao X J. 2011. Long-term visibility trends and characteristics in the region of Beijing, Tianjin, 405 and Hebei, China. *Atmospheric Research*. 101(3): 711–718.

### Tables and Figures captions:

**Table 1.** Correlation coefficients between  $WHD_{NCP}$  and three teleconnection (EA/WR, WP and EU) indices. A single asterisk (\*) indicates that the result exceeded the 95% confidence level, and double asterisks (\*\*) indicate that it exceeded the 99% confidence level. Note: OS means ‘original sequence’, and ‘detrended’ means that the linear trend was removed.

410 **Table 2.** Summary of the various influence factors for  $WHD_{NCP}$ . The “+++” indicates “more important”; “++” indicates “important”, “+” indicates “less important”, and blank indicates “not important”.

**Figure 1.** Topographic map (shading; unit: m) of North China and the locations of 39 NCP observation sites (Urban: black circle, Rural: white circle). The NCP area is represented by a black rectangle, and the names of provinces and mountains are written in red and white, respectively.

415 ~~**Figure 2.** Visibility of Beijing (green) and atmospheric compositions at BaoLian (blue) and Shangdianzi (red) stations at 02:00, 08:00, 14:00 and 20:00 LT from 1<sup>st</sup> Dec 2014 to 28<sup>th</sup> Feb 2015. The eight compositions included here are  $SO_2$ ,  $NO$ ,  $NO_2$ ,  $NO_x$ ,  $CO$ ,  $O_3$ ,  $PM_{2.5}$  and NEP from top to bottom. The correlation coefficient was recorded as “CC”, and the “N” denotes the number of composition samples. The total number of visibility observations was 360, which was adjusted to match the “N” of each composition after quality control and to compute CC.~~

420 **Figure 32.** Variation of  $WHD_{NCP}$  from 1979–2014 (Units: days), the error bar represents one standard error among the measured sites. For 2013–2014, the thresholds of 7.5 km (blue) and 10 km (gray) are both shown, and the dashed lines indicate the mean values for 1979–1992 and 1993–2012, respectively.

**Figure 43.** Distributions of WHD from 1979 to 2012 (a) and anomalies in 2014 relative to 1979-2012 (b).

**Figure 54.** Correlation coefficients between  $WHD_{NCP}$  and winter circulations from 1979 to 2012 with linear trend was removed (a, be), and circulation anomalies in 2014 (bc, d) and 2010 (e, f). The circulations in (a, c, eb) are TS (shade) and SLP (contour) and those in (c, d, f) are surface wind speed (shade) and wind vector (arrow).

**Figure 65.** Correlation coefficients between  $WHD_{NCP}$  and winter H500 (a) / UV850 (b) from 1979 to 2012. The linear trend was removed, and shade indicates that CC exceeds the 95% confidence level. UV850 (arrow) and speed (shade) anomalies in winter 2014 (c) and 2010 (d). A and C represent anti-cyclone and cyclone, respectively.

**Figure 6.** The difference of winter PBLH between 2014 and 2010

**Figure 77.** Heterogeneous correlation map of the first SVD model for detrended and normalized (a) H500 during DJF and (b) ASI during SON 1979–2014; (c) ASI anomaly during SON 2014. A and C represent anti-cyclone and cyclone, respectively.

**Figure 88.** Heterogeneous correlation map of the first SVD model for detrended and normalized (a) H500 during DJF and (b) TS during DJF 1979–2014; (c) TS anomaly during DJF 2014. A and C represent anti-cyclone and cyclone, respectively.

**Figure 99.** Heterogeneous correlation map of the first SVD model for detrended and normalized (a) H500 during DJF and (b) SST during ON 1979–2014; (c) SST anomaly during ON 2014. A and C represent anti-cyclone and cyclone, respectively.

**Figure 1010.** Heterogeneous correlation map of the second SVD model for detrended and normalized (a) H500 during DJF and (b) TS during SON 1979–2014; (c) TS anomaly during SON 2014. A and C represent anti-cyclone and cyclone, respectively.

**Figure 1111.** Mean mass concentration of  $PM_{2.5}$  in winter at Shangdianzi Station from 2004 to 2014 as measured by the TOEM (solid) and  $\beta$ -ray (dash) method. The error bar represents one standard error among the different measured hours.

**Figure S1.** Visibility of Beijing (green) and atmospheric compositions at BaoLian (blue) and Shangdianzi (red) stations at 02:00, 08:00, 14:00 and 20:00 LT from 1<sup>st</sup> Dec 2014 to 28<sup>th</sup> Feb 2015. The eight compositions included here are  $SO_2$ ,  $NO$ ,  $NO_2$ ,  $NO_x$ ,  $CO$ ,  $O_3$ ,  $PM_{2.5}$  and NEP from top to bottom. The correlation coefficient was recorded as “CC”, and the “N” denotes the number of composition samples. The total number of visibility observations was 360, which was adjusted to match the “N” of each composition after quality control and to compute CC.

Figure S1S2. Anomalies of pre-autumn ASI in 2010

Figure S2S3. Anomalies of winter TS in 2010

Figure S3S4. Anomalies of ON SST in 2010

450 Figure S4S5. Anomalies of pre-autumn TS in 2010

Figure S5S6. UV850 (arrow) and speed (shade) anomalies in 2013. A and C represent anti-cyclone and cyclone, respectively.

[Figure S7. Anomalies of surface wind speed \(contour\) and PBLH \(shade\) in winter 2013](#)

455 Figure S6S8. Anomalies of external forcings in 2013. (a) ASI in pre-autumn, (b) TS in winter, (c) SST in Oct and Nov, and (d) TS in pre-autumn.

Figure S7S9. Correlation coefficients between EA/WR index and H500 (a) / Atlantic SST in pre-autumn (b). Pre-autumn SST anomaly during SON in 2013 (c) and 2014 (d)

460

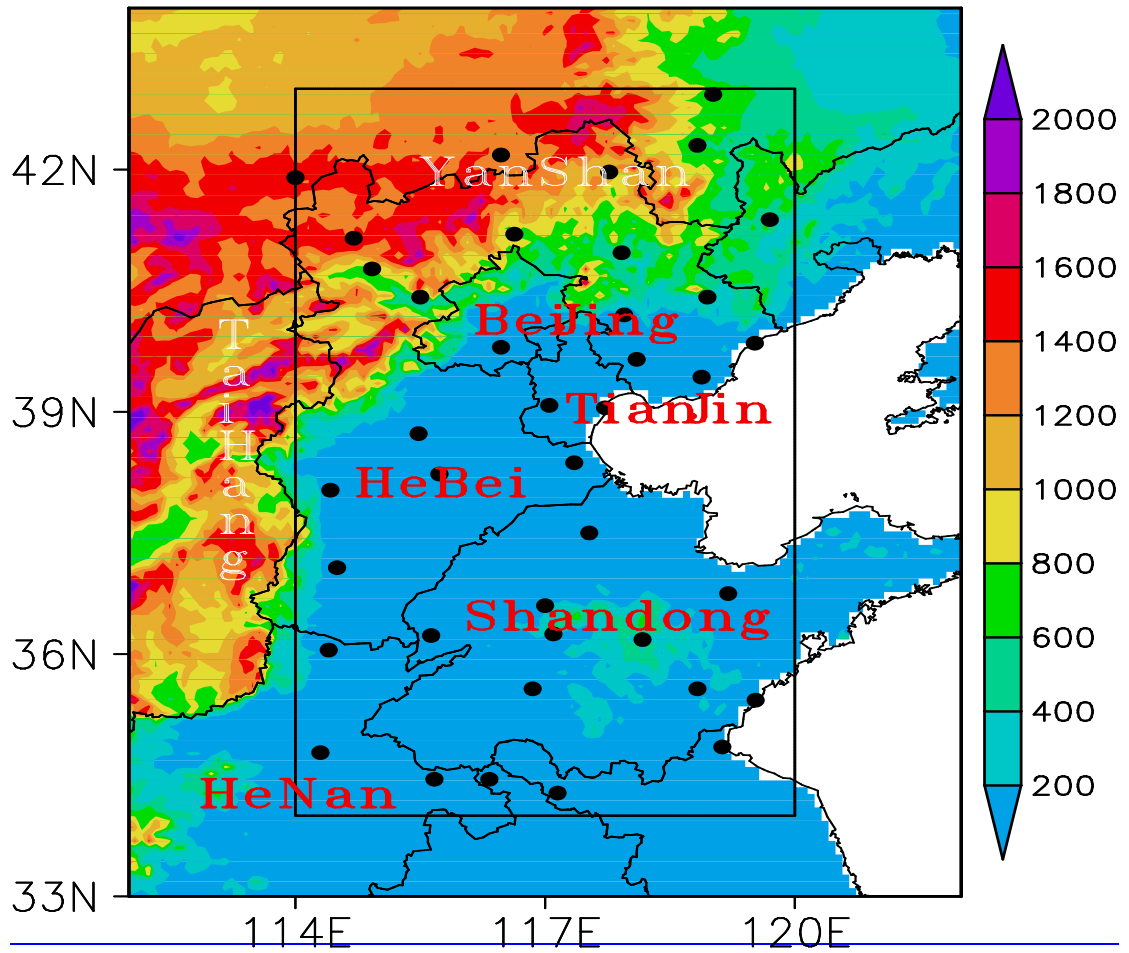
**Table 1. Correlation coefficients between  $WHD_{NCP}$  and three teleconnection (EA/WR, WP and EU) indices. A single asterisk (\*) indicates that the result exceeded the 95% confidence level, and double asterisks (\*\*) indicate that it exceeded the 99% confidence level. Note: OS means ‘original sequence’, and ‘detrended’ means that the linear trend was removed.**

<i>Pattern</i>	<i>OS</i>	<i>Detrended</i>
EA/WR	0.36*	0.43**
WP	-0.06	0.41*
EU	0.34*	-0.13

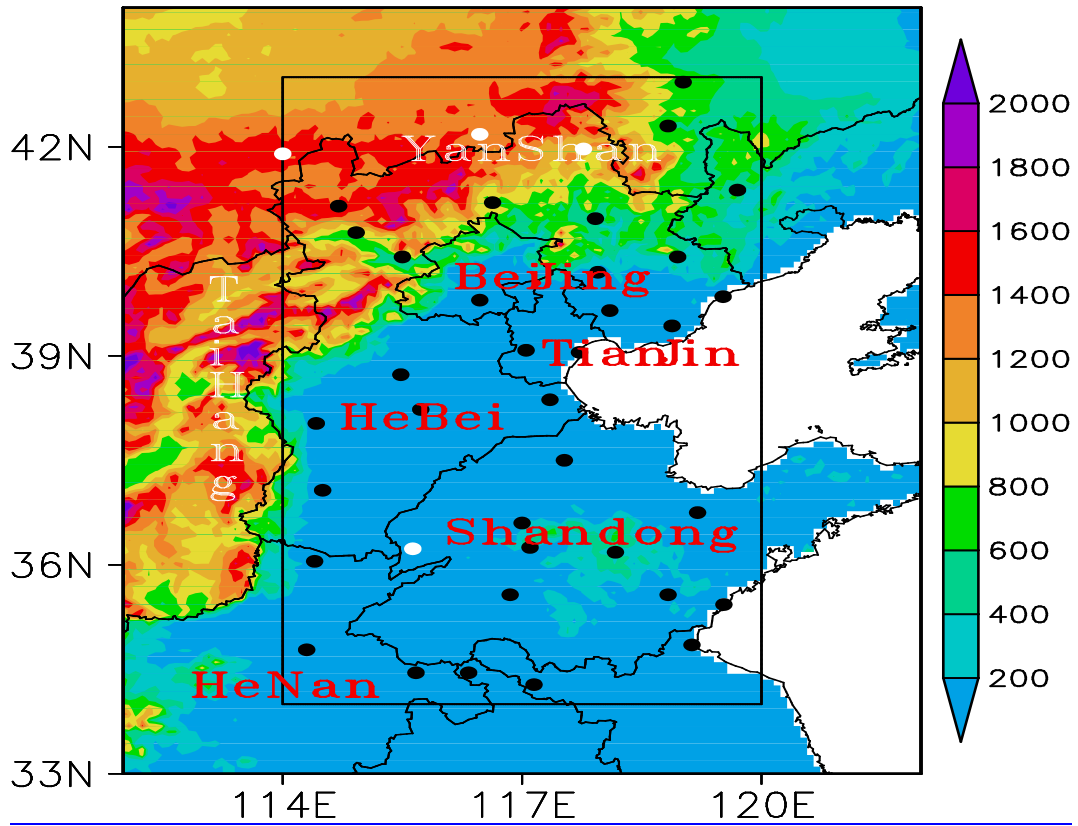
465

Table 2. Summary of the various influence factors for WHD<sub>NCP</sub>. The “+++” indicates “more important”; “++” indicates “important”, “+” indicates “less important”, and blank indicates “not important”.

<i>Factors</i>	<i>2010</i>	<i>2013</i>	<i>2014</i>
<u>PM<sub>2.5</sub> concentration</u>	++	+++	++
<u>Local surface wind speed</u>	++	++	++
<u>Local PBLH</u>	++	++	++
EA/WR	++	++	++
WP	++		++
EU			++
<u>PM<sub>2.5</sub> concentration</u>	++	+++	++
Pre-autumn ASI	++		++
Winter TS	++		++
ON Pacific SSTA	+	++	++
Pre-autumn TS	++		++
SON Atlantic SSTA		++	



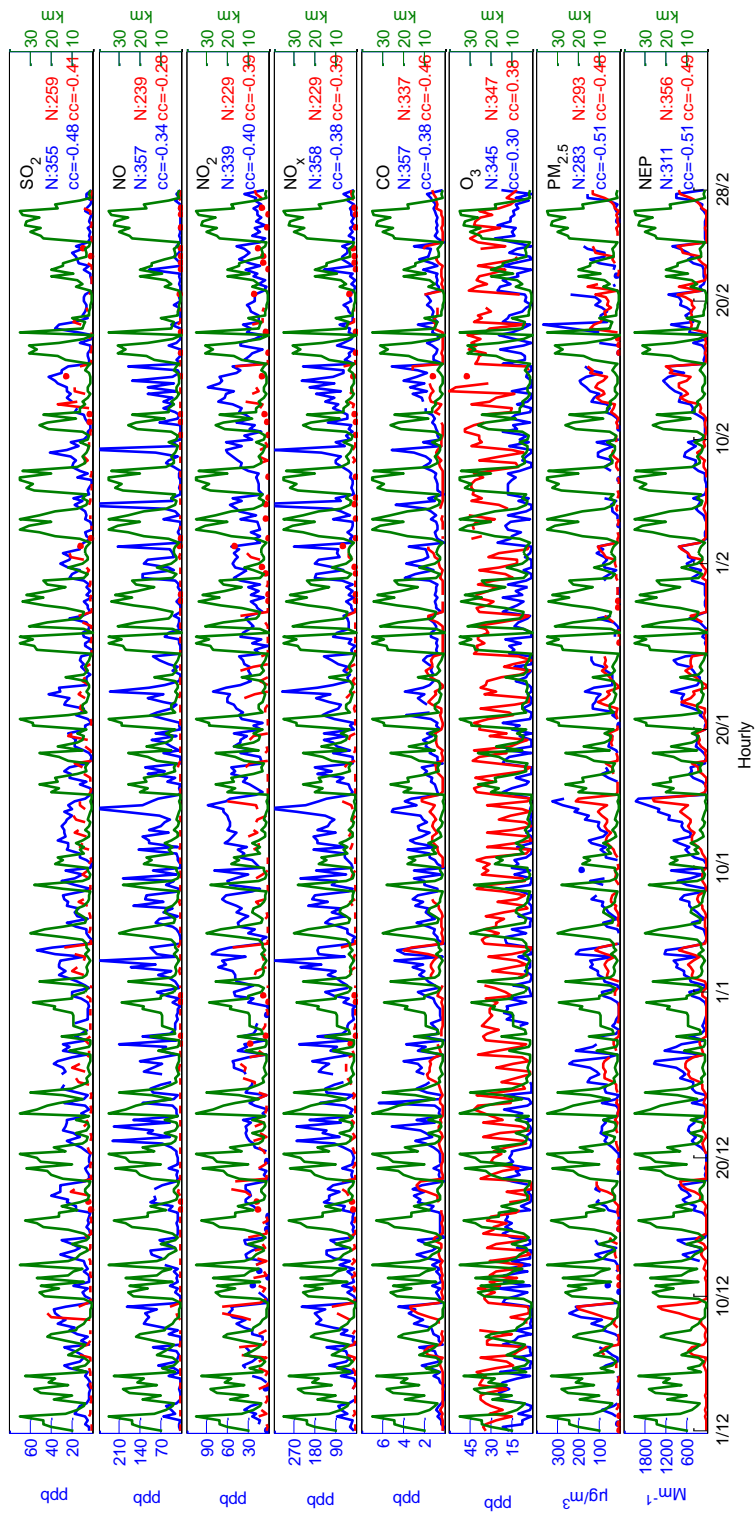




475

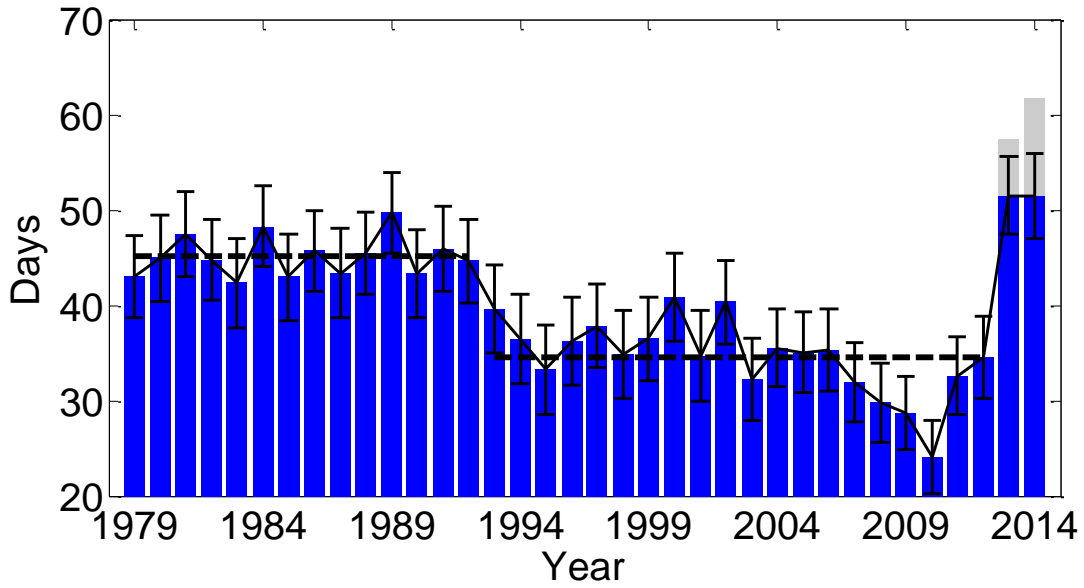
Figure 1. Topographic map (shading; unit: m) of North China and the locations of 39 NCP observation sites (Urban: black circle, Rural: white circle). The NCP area is represented by a black rectangle, and the names of provinces and mountains are written in red and white, respectively.

480



485

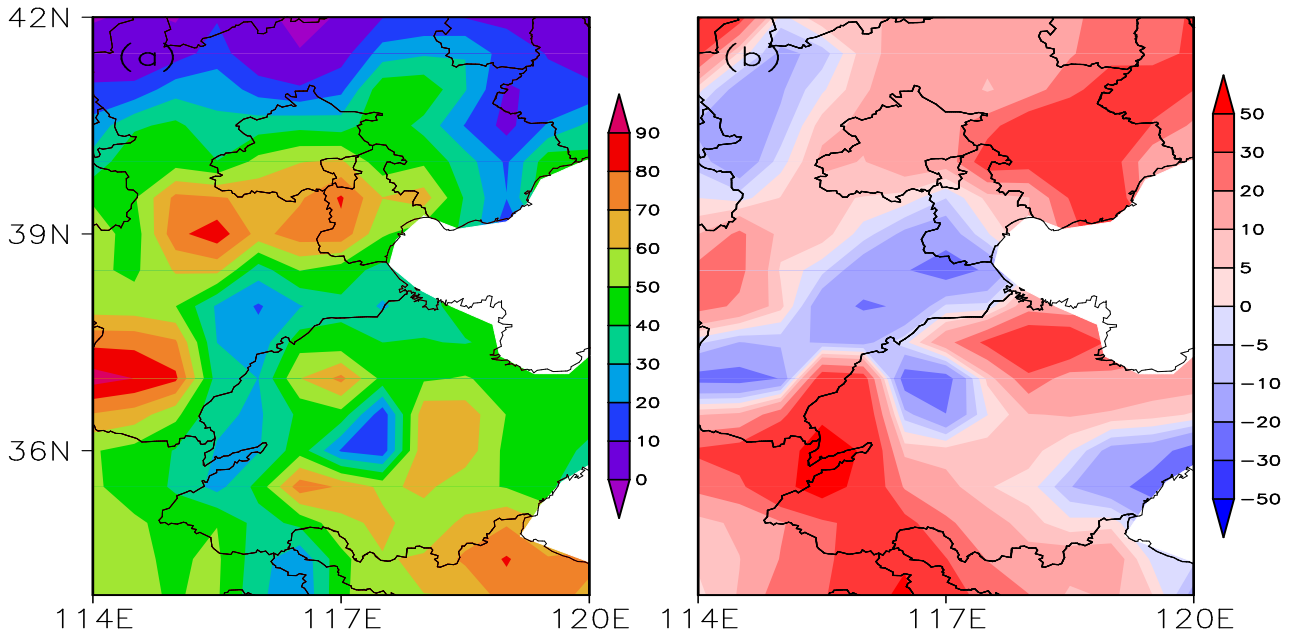
Figure 2.— Visibility of Beijing (green) and atmospheric compositions at BaoLian (blue) and Shangdianzi (red) stations at 02:00, 08:00, 14:00 and 20:00 LT from 1<sup>st</sup> Dec 2014 to 28<sup>th</sup> Feb 2015. The eight compositions included here are SO<sub>2</sub>, NO, NO<sub>2</sub>, NO<sub>x</sub>, CO, O<sub>3</sub>, PM<sub>2.5</sub> and NEP from top to bottom. The correlation coefficient was recorded as “CC”, and the “N” denotes the number of composition samples. The total number of visibility observations was 360, which was adjusted to match the “N” of each composition after quality control and to compute CC.



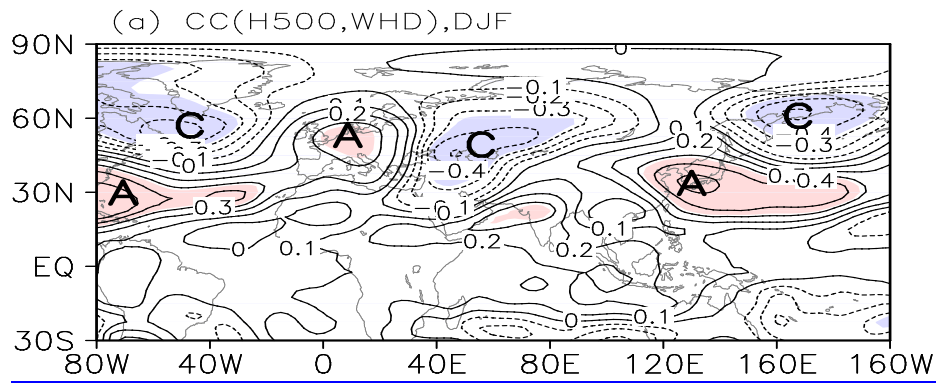
490

Figure 32. Variation of WHD<sub>NCP</sub> from 1979–2014 (Units: days), the error bar represents one standard error among the measured sites. For 2013–2014, the thresholds of 7.5 km (blue) and 10 km (gray) are both shown, and the dashed lines indicate the mean values for 1979–1992 and 1993–2012, respectively.

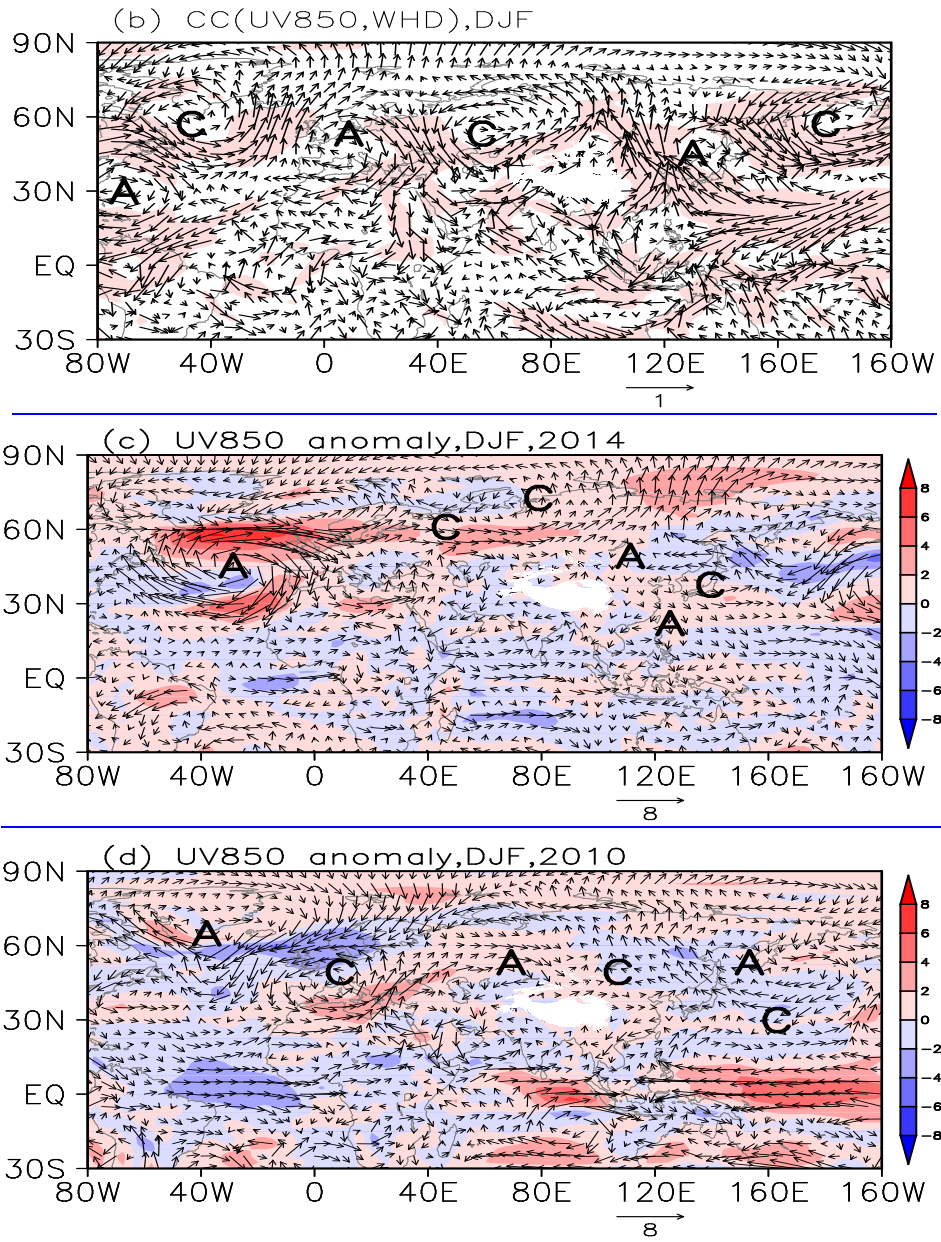
495



**Figure 43.** Distributions of WHD from 1979 to 2012 (a) and anomalies in 2014 relative to 1979-2012 (b).

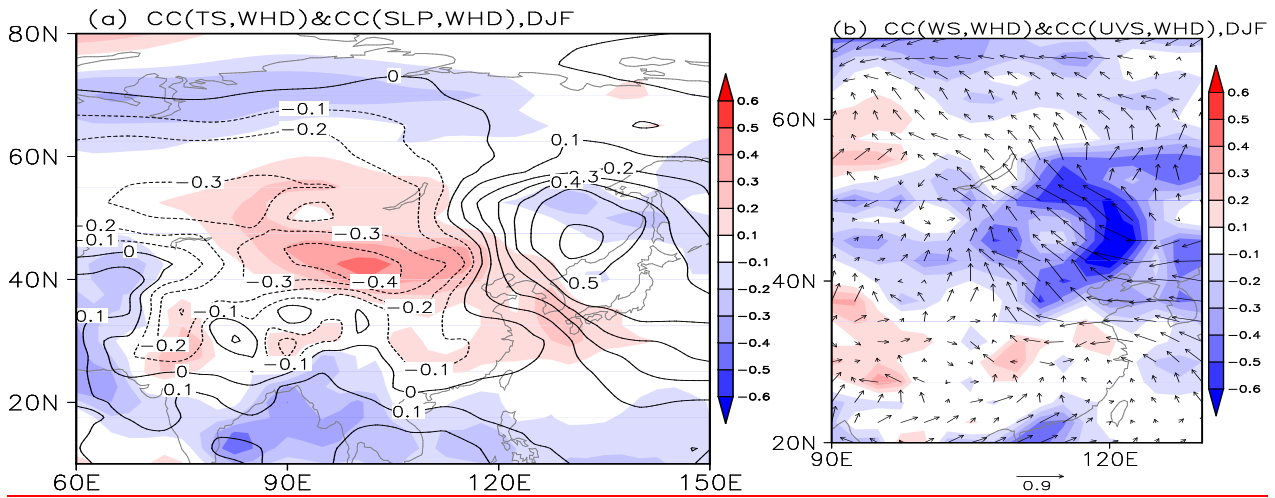
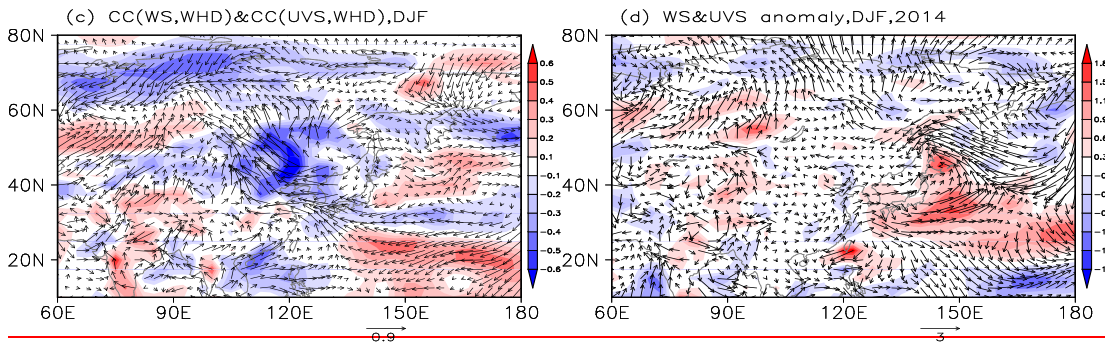
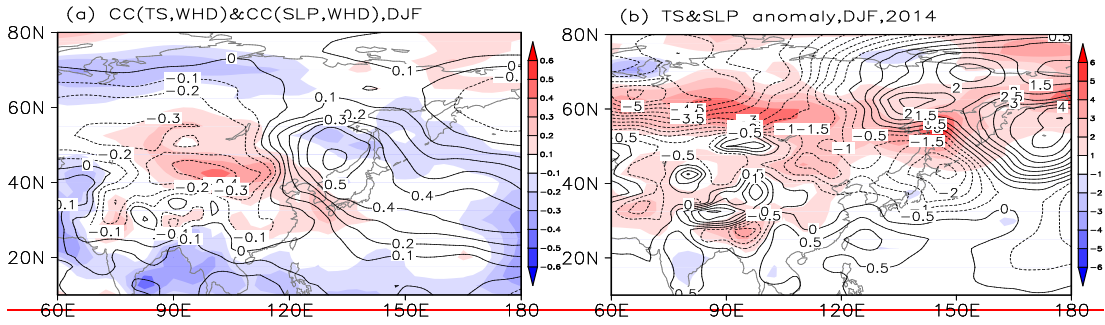


500

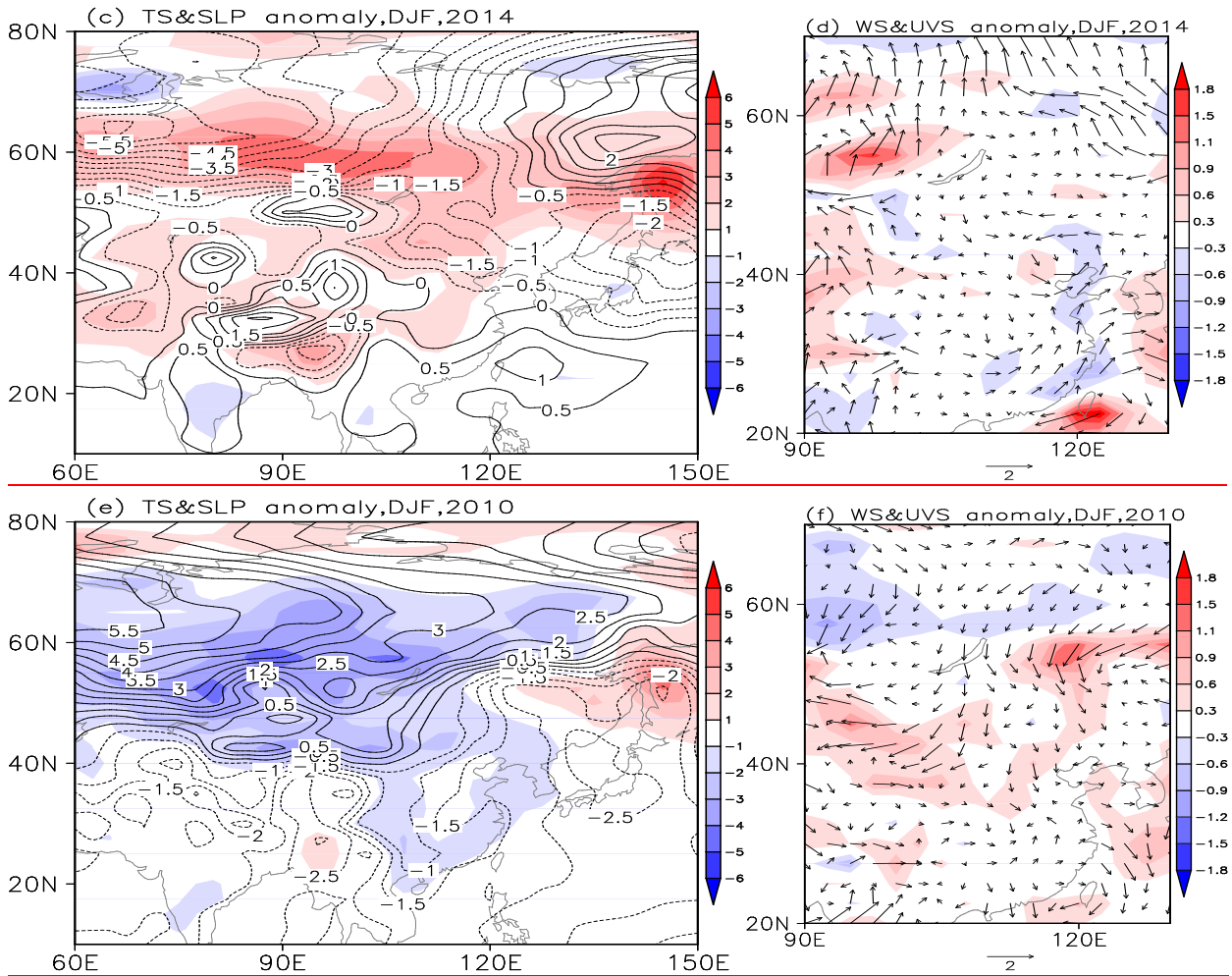


**Figure 4. Correlation coefficients between  $WHD_{NCP}$  and winter H500 (a) / UV850 (b) from 1979 to 2012. The linear trend was removed, and shade indicates that CC exceeds the 95% confidence level. UV850 (arrow) and speed (shade) anomalies in winter 2014 (c) and 2010 (d). A and C represent anti-cyclone and cyclone, respectively.**

505

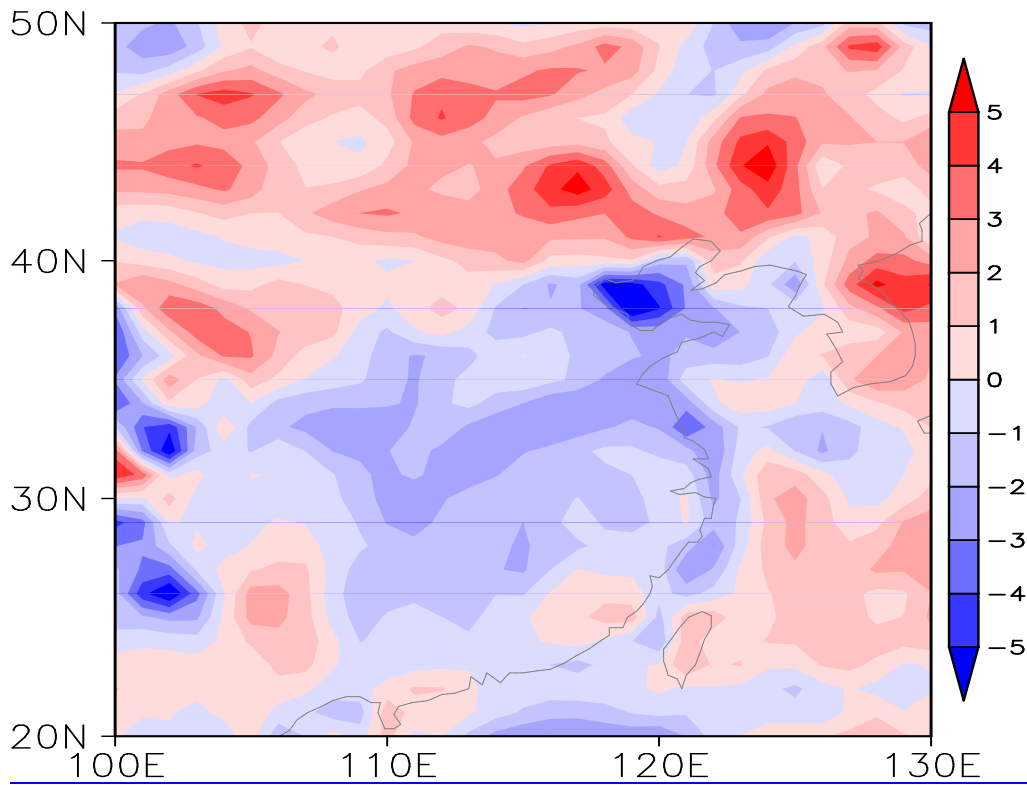






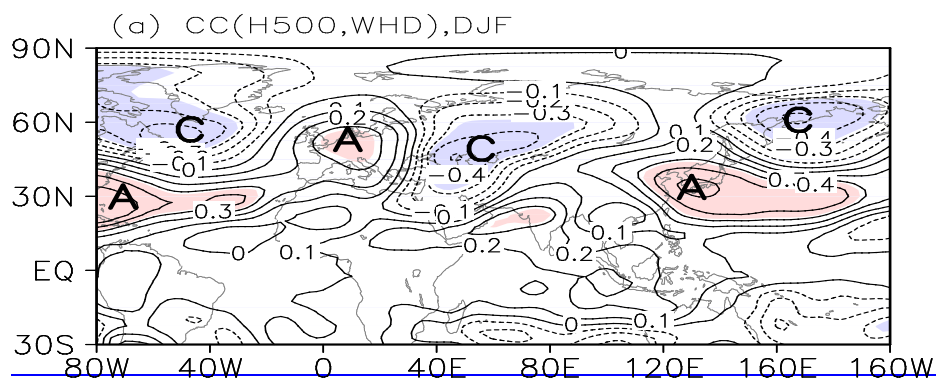
**Figure 545.** Correlation coefficients between  $WHD_{NCP}$  and winter circulations from 1979 to 2012 with linear trend was removed (a, eb), and circulation anomalies in 2014 (bc, d) and 2010 (e, f). The circulations in (a, c, eb) are TS (shade) and SLP (contour) and those in (c, d, f) are surface wind speed (shade) and wind vector (arrow).

515



**Figure 6. The difference of winter PBLH between 2014 and 2010**

520





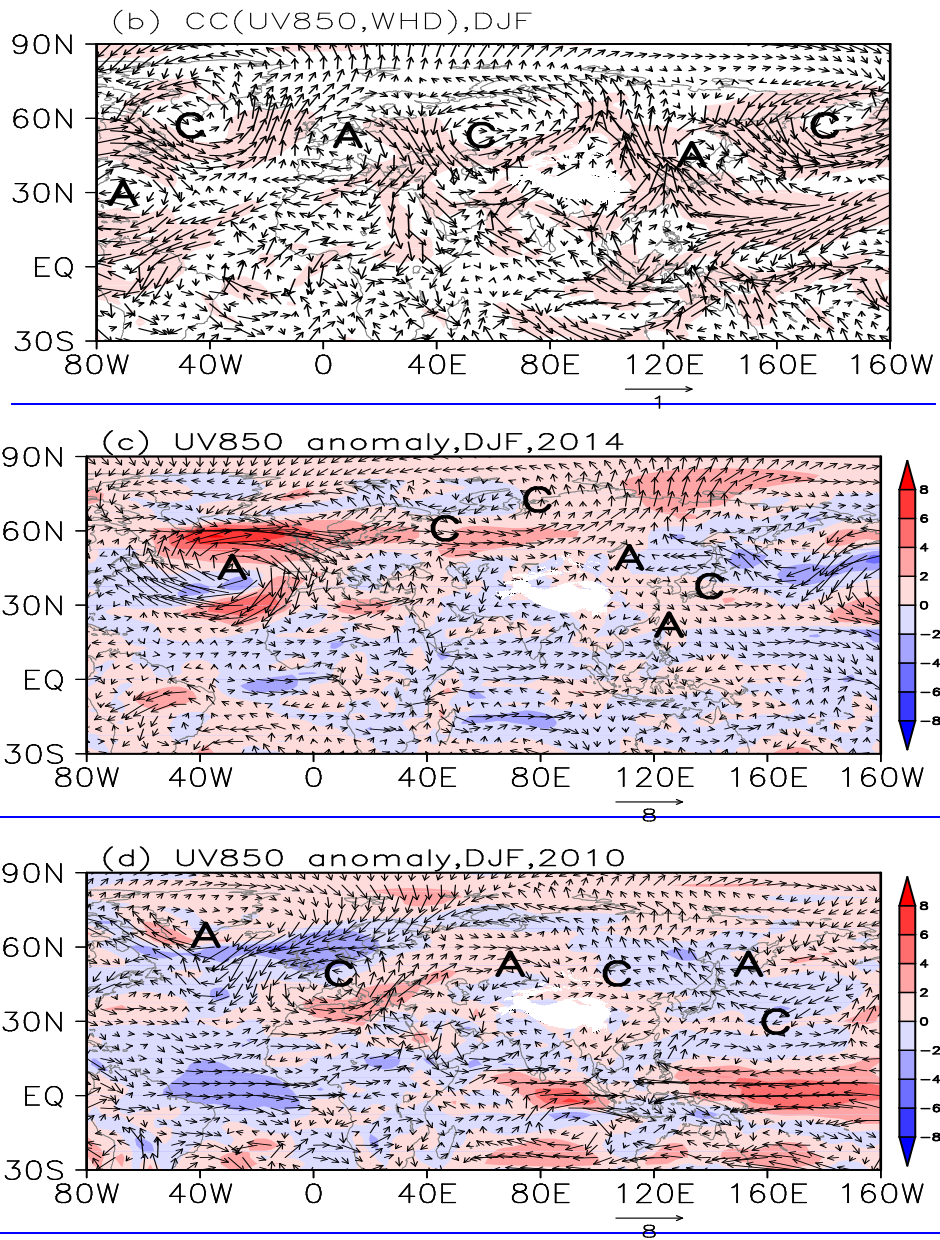
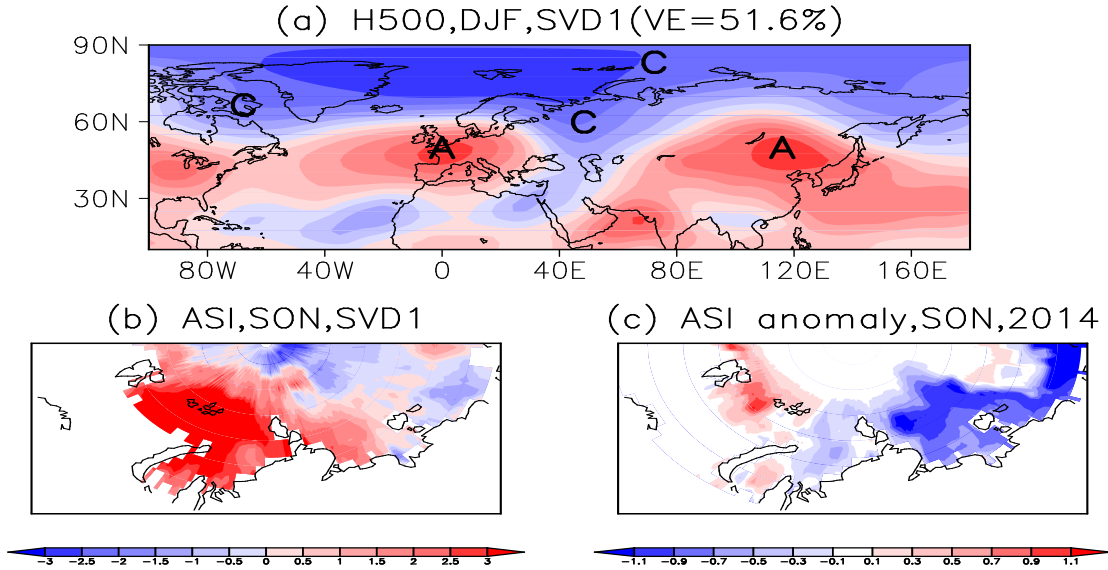


Figure 65. Correlation coefficients between  $WHD_{NCP}$  and winter H500 (a) / UV850 (b) from 1979 to 2012. The linear trend was removed, and shade indicates that CC exceeds the 95% confidence level. UV850 (arrow) and speed (shade) anomalies in winter 2014 (c) and 2010 (d). A and C represent anti-cyclone and cyclone, respectively.

525

530



**Figure 767.** Heterogeneous correlation map of the first SVD model for detrended and normalized (a) H500 during DJF and (b) ASI during SON 1979–2014; (c) ASI anomaly during SON 2014. A and C represent anti-cyclone and cyclone, respectively.

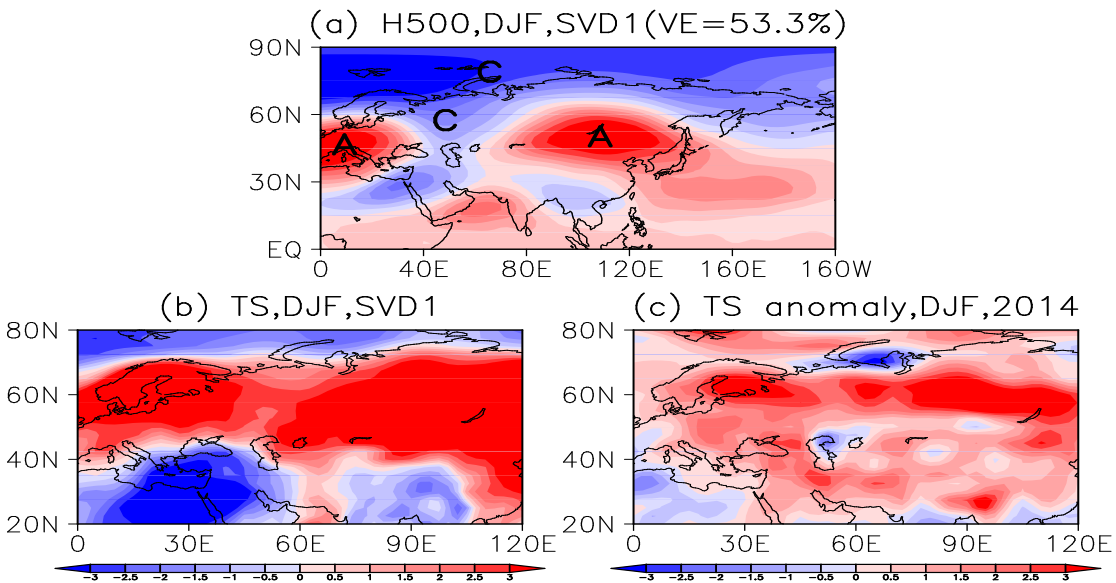
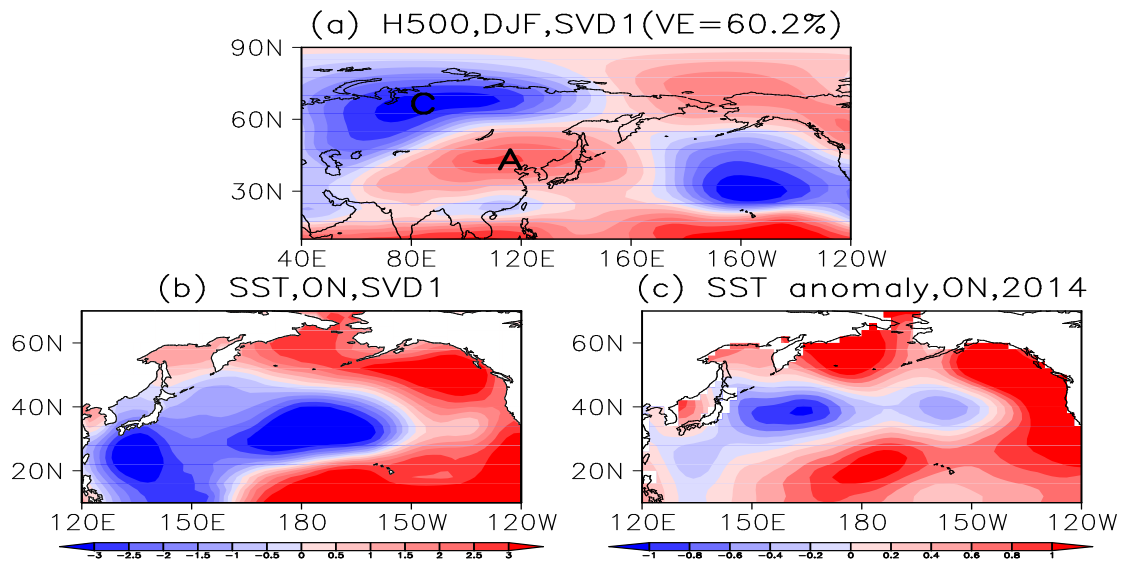


**Figure 878.** Heterogeneous correlation map of the first SVD model for detrended and normalized (a) H500 during DJF and (b) TS during DJF 1979–2014; (c) TS anomaly during DJF 2014. A and C represent anti-cyclone and cyclone, respectively.

540



545

**Figure 989.** Heterogeneous correlation map of the first SVD model for detrended and normalized (a) H500 during DJF and (b) SST during ON 1979–2014; (c) SST anomaly during ON 2014. A and C represent anti-cyclone and cyclone, respectively.

550

555

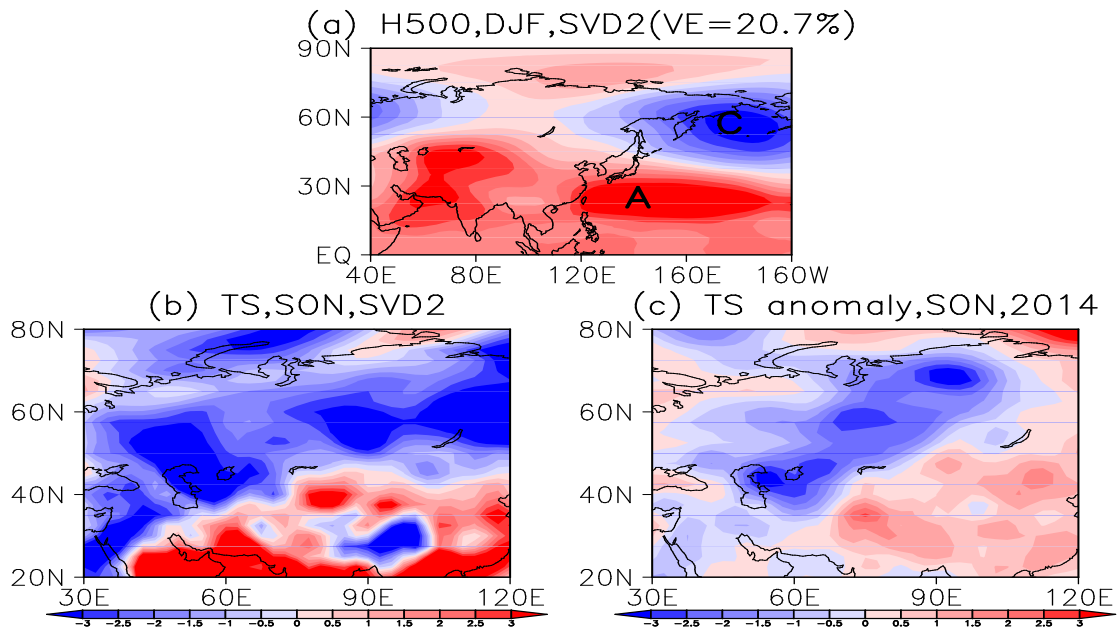


**Figure 10910.** Heterogeneous correlation map of the second SVD model for detrended and normalized (a) H500 during DJF and (b) TS during SON 1979–2014; (c) TS anomaly during SON 2014. A and C represent anti-cyclone and cyclone, respectively.

560

565

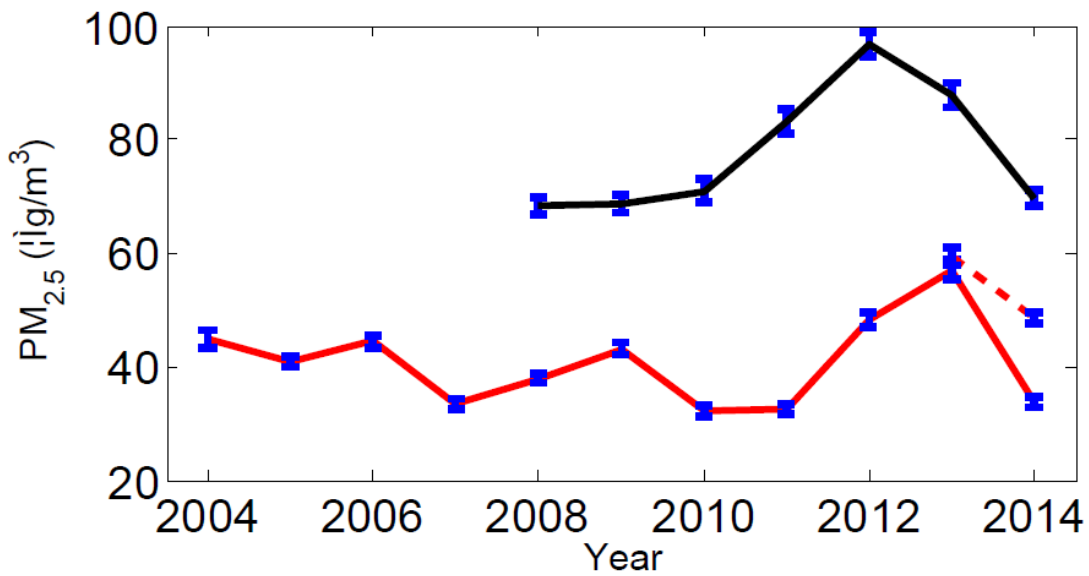
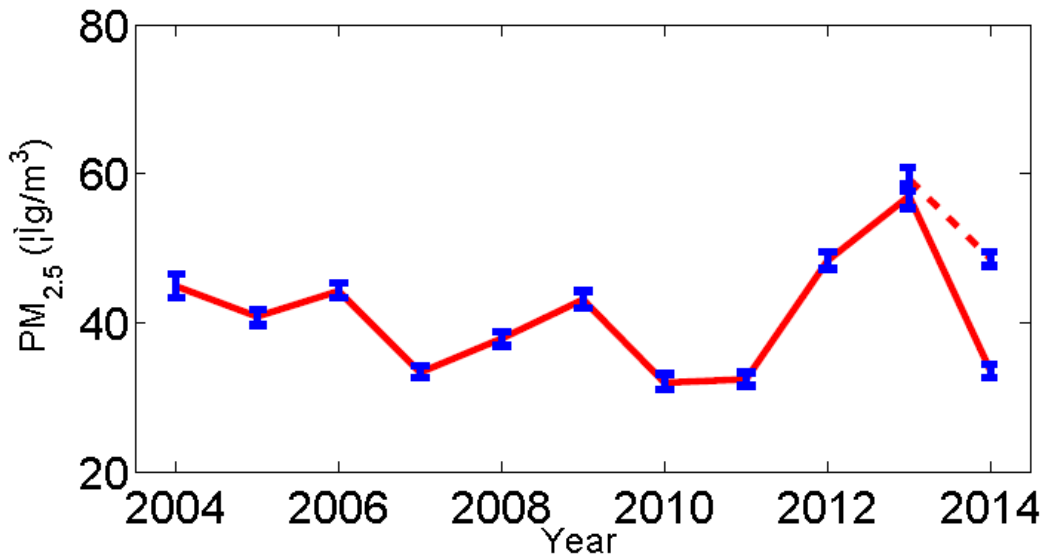


Figure 4-10-11. Mean mass concentration of PM<sub>2.5</sub> in winter at Shangdianzi (red; measured by the TOEM (solid) and β-ray (red dash) method) and Baolian (black) Station, from 2004 to 2014 as measured by the TOEM (solid) and β-ray (dash) method. The error bar represents one standard error among the different measured hours.

570

## Supplemental Materials

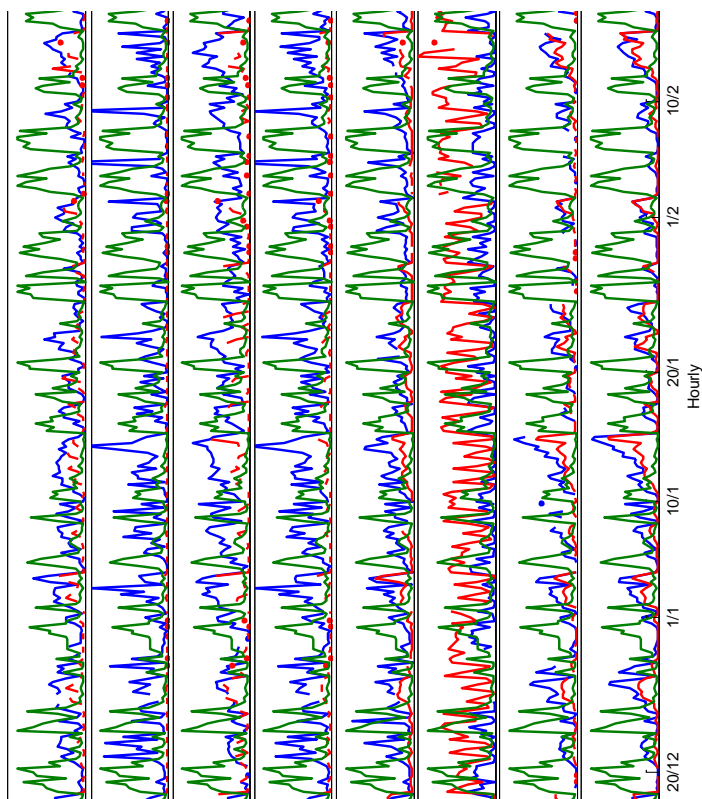
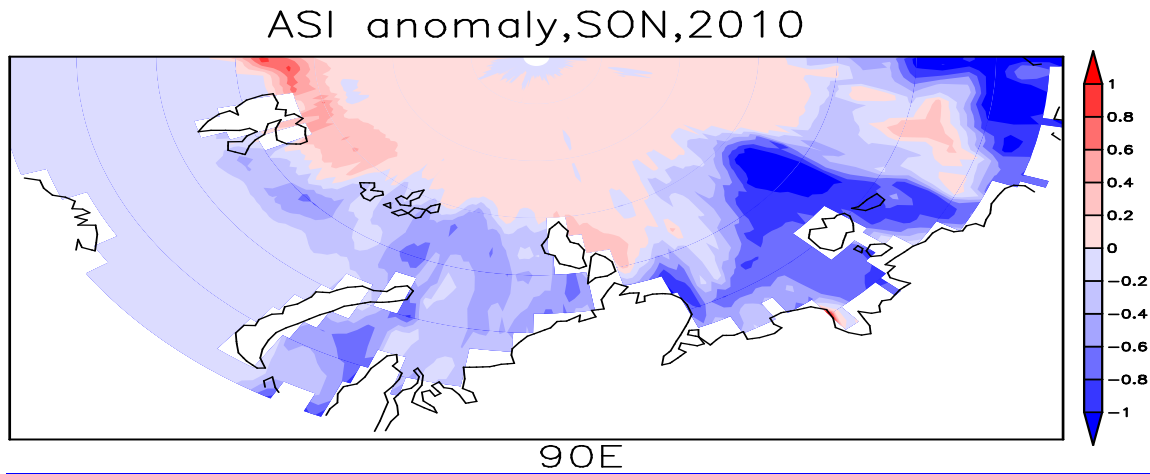
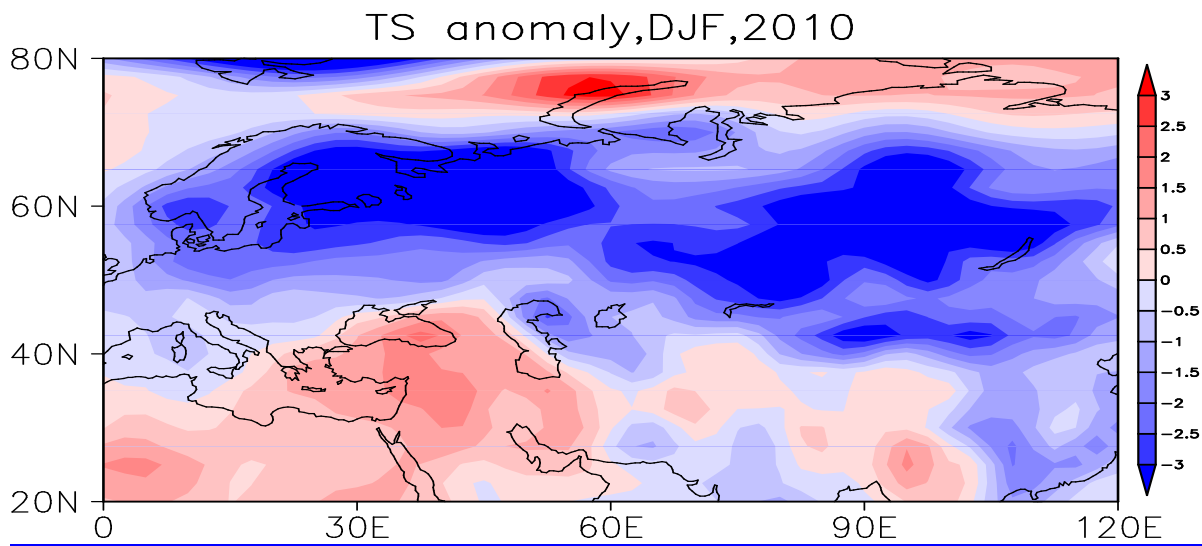


Figure S1. Visibility of Beijing (green) and atmospheric compositions at BaoLian (blue) and Shangdianzi (red) stations at 02:00, 08:00, 14:00 and 20:00 LT from 1<sup>st</sup> Dec 2014 to 28<sup>th</sup> Feb 2015. The eight compositions included here are SO<sub>2</sub>, NO, NO<sub>2</sub>, NO<sub>3</sub>, CO, O<sub>3</sub>, PM<sub>2.5</sub> and NEP from top to bottom. The correlation coefficient was recorded as “CC”, and the “N” denotes the number of composition samples. The total number of visibility observations was 360, which was adjusted to match the “N” of each composition after quality control and to compute CC.



**Figure S2. Anomalies of pre-autumn ASI in 2010**



**Figure S3. Anomalies of winter TS in 2010**

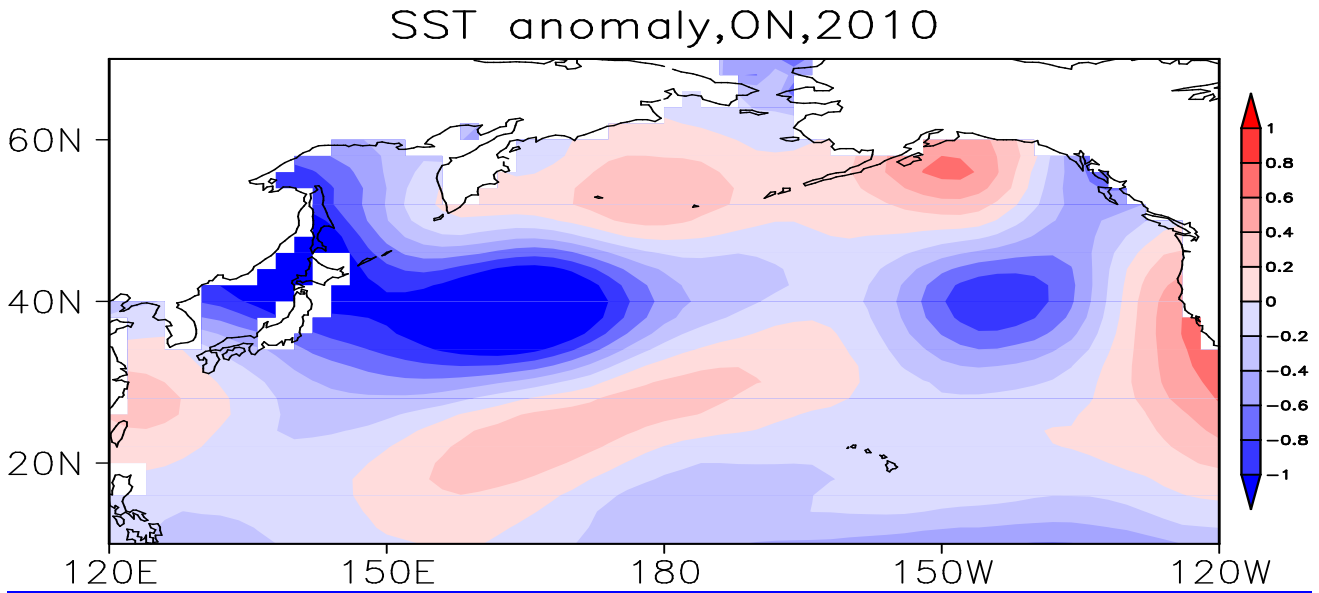


[Figure S4. Anomalies of ON SST in 2010](#)

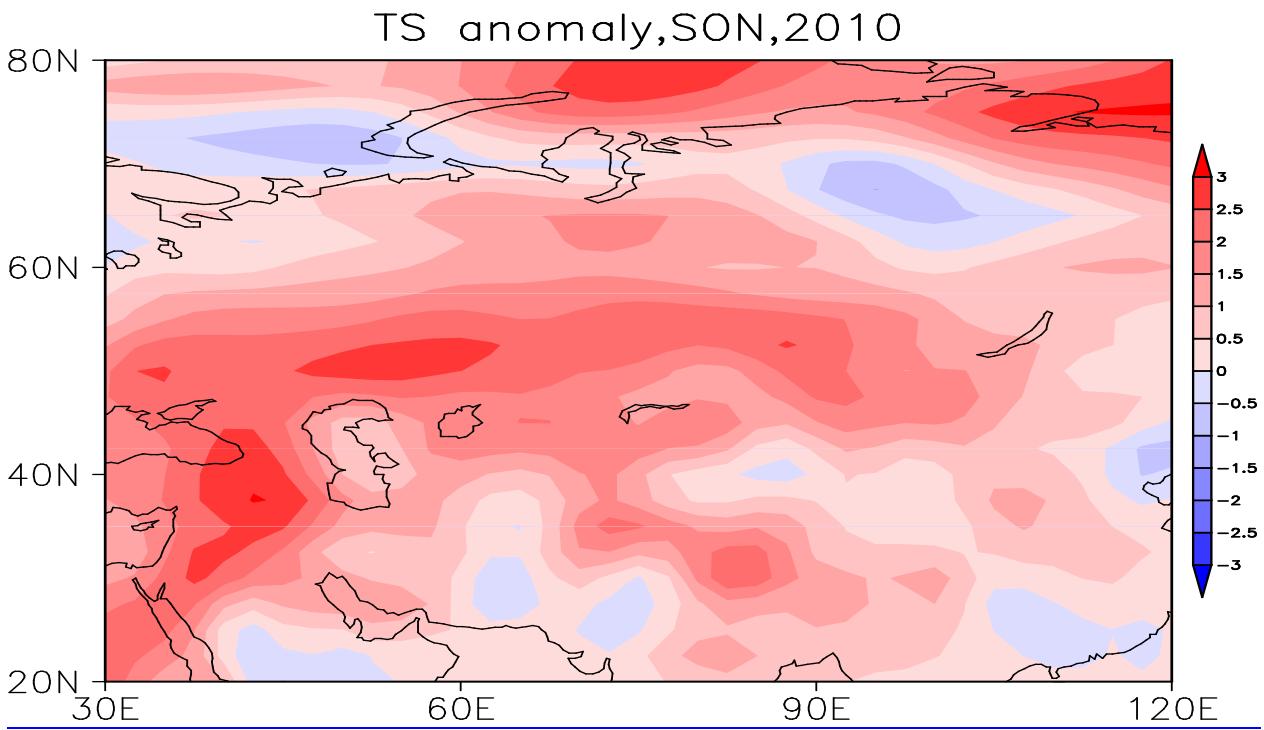


[Figure S5. Anomalies of pre-autumn TS in 2010](#)

590



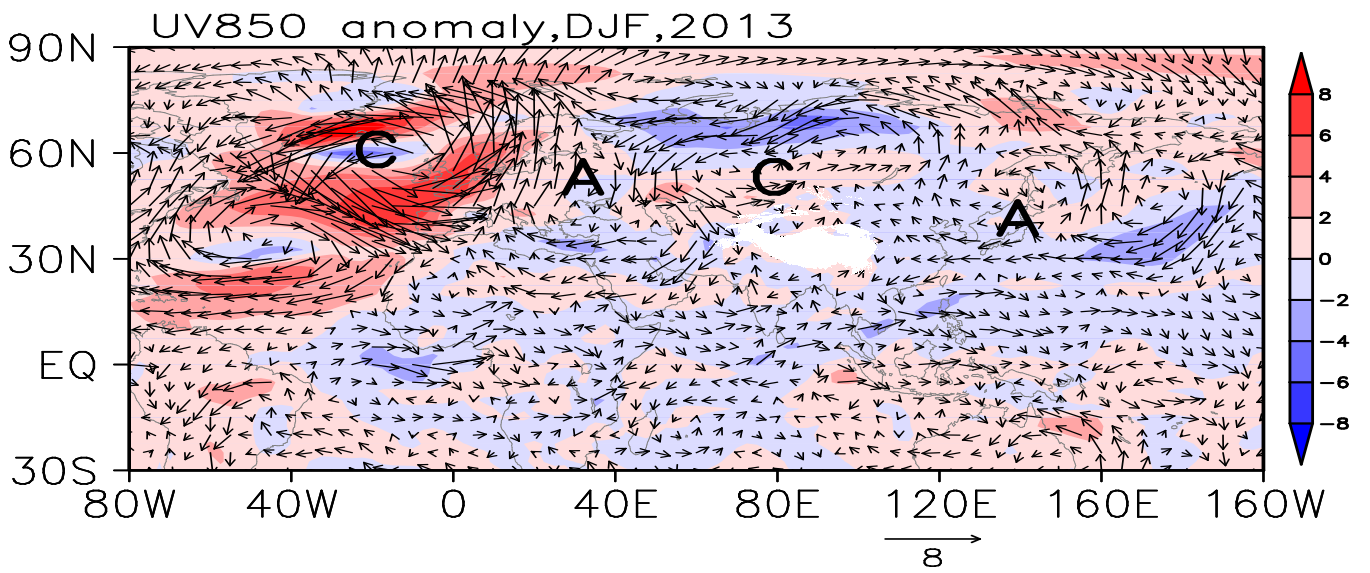


Figure S6. UV850 (arrow) and speed (shade) anomalies in 2013. A and C represent anti-cyclone and cyclone, respectively.

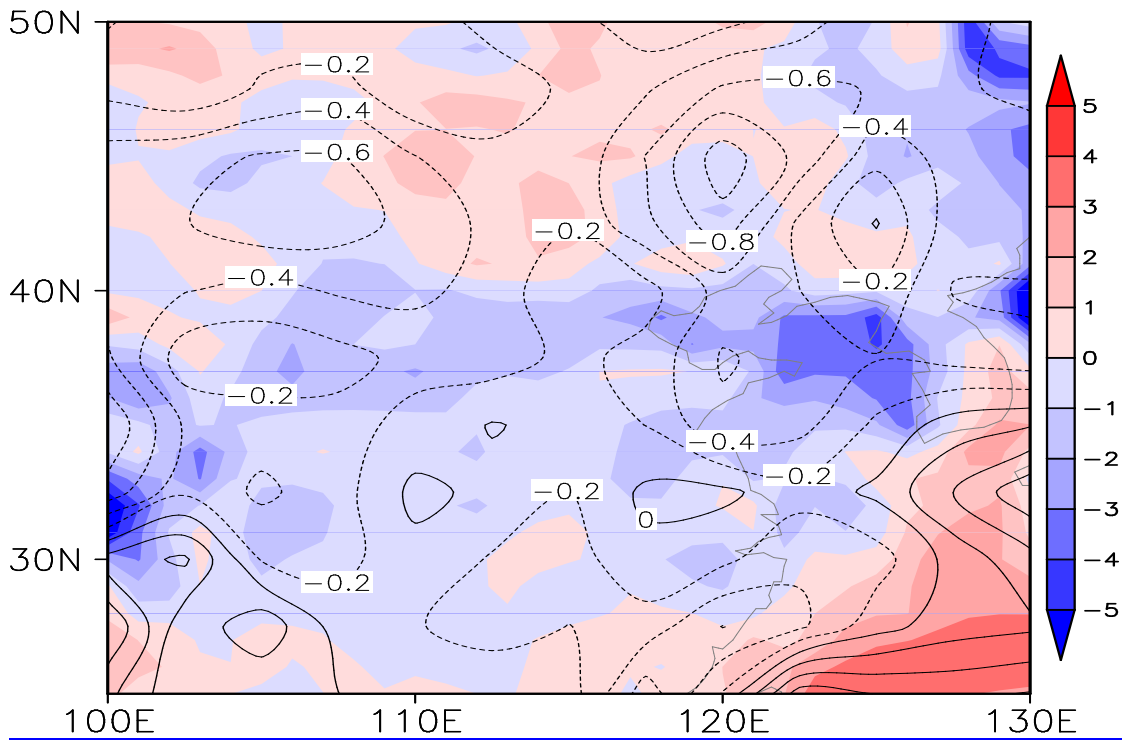
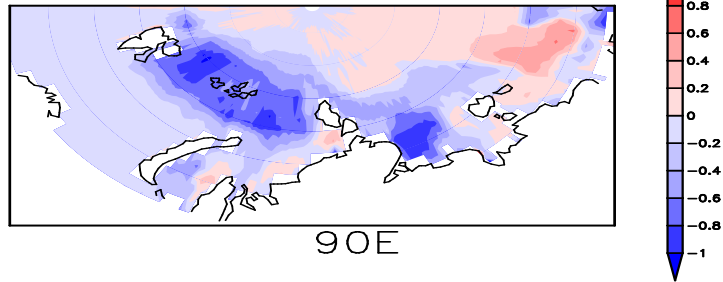


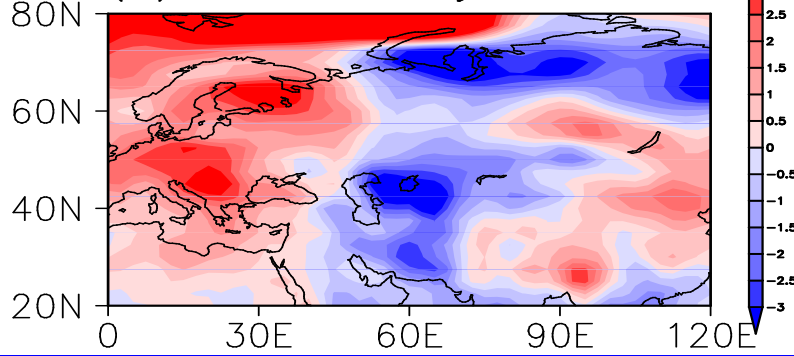
Figure S7. Anomalies of surface wind speed (contour) and PBLH (shade) in winter 2013

595

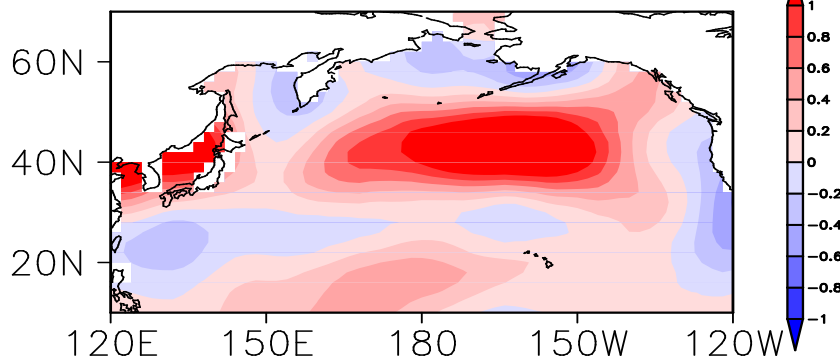
(a) ASI anomaly, SON, 2013

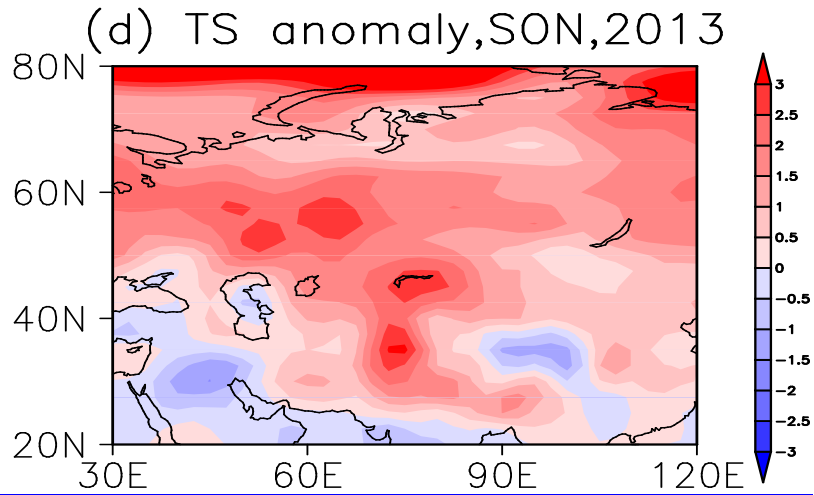


(b) TS anomaly, DJF, 2013



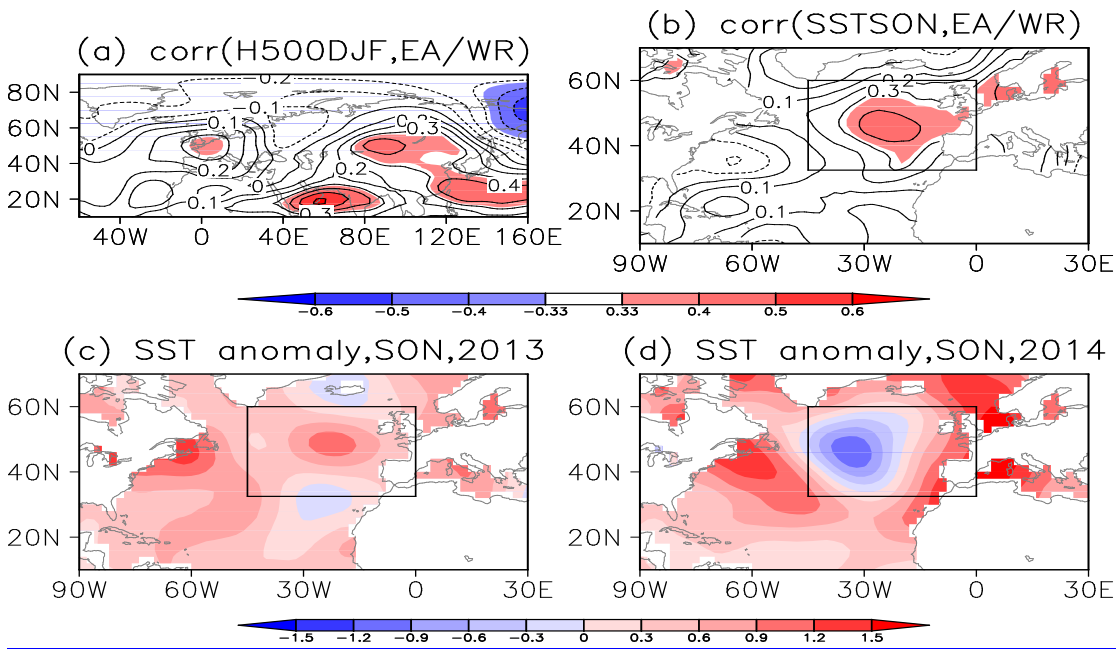
(c) SST anomaly, ON, 2013





600

**Figure S8. Anomalies of external forcings in 2013. (a) ASI in pre-autumn, (b) TS in winter, (c) SST in Oct and Nov, and (d) TS in pre-autumn.**



605

**Figure S9. Correlation coefficients between EA/WR index and H500 (a) / Atlantic SST in pre-autumn (b). Pre-autumn SST anomaly during SON in 2013 (c) and 2014 (d)**

